




# An Interactive Generic Physiologically Based Pharmacokinetic (igPBPK) Modeling Platform to Predict Drug Withdrawal Intervals in Cattle and Swine: A Case Study on Flunixin, Florfenicol, and Penicillin G

Wei-Chun Chou <sup>\*,†</sup> Lisa A. Tell,<sup>‡</sup> Ronald E. Baynes,<sup>§</sup> Jennifer L. Davis <sup>,¶</sup> Fiona P. Maunsell,<sup>||</sup> Jim E. Riviere,<sup>§,|||</sup> and Zhoumeng Lin <sup>\*,†,1</sup>

<sup>\*</sup>Department of Environmental and Global Health, College of Public Health and Health Professions, University of Florida, Gainesville, Florida 32610, USA; <sup>†</sup>Center for Environmental and Human Toxicology, University of Florida, Florida 32608, USA; <sup>‡</sup>Department of Medicine and Epidemiology, School of Veterinary Medicine, University of California-Davis, Davis, California 95616, USA; <sup>§</sup>Center for Chemical Toxicology Research and Pharmacokinetics, Department of Population Health and Pathobiology, College of Veterinary Medicine, North Carolina State University, Raleigh, North Carolina 27606, USA; <sup>¶</sup>Department of Biomedical Sciences and Pathobiology, Virginia-Maryland College of Veterinary Medicine, Blacksburg, Virginia 24060, USA; <sup>||</sup>Department of Large Animal Clinical Sciences, College of Veterinary Medicine, University of Florida, Gainesville, Florida 32608, USA; and <sup>|||</sup>1Data Consortium, Kansas State University, Olathe, Kansas 66061, USA

<sup>1</sup>To whom correspondence should be addressed at Department of Environmental and Global Health, College of Public Health and Health Professions, University of Florida, 1225 Center Drive, Gainesville, Florida 32610, USA. E-mail: [linzhoumeng@ufl.edu](mailto:linzhoumeng@ufl.edu).

## ABSTRACT

Violative chemical residues in edible tissues from food-producing animals are of global public health concern. Great efforts have been made to develop physiologically based pharmacokinetic (PBPK) models for estimating withdrawal intervals (WDIs) for extralabel prescribed drugs in food animals. Existing models are insufficient to address the food safety concern as these models are either limited to 1 specific drug or difficult to be used by non-modelers. This study aimed to develop a user-friendly generic PBPK platform that can predict tissue residues and estimate WDIs for multiple drugs including flunixin, florfenicol, and penicillin G in cattle and swine. Mechanism-based *in silico* methods were used to predict tissue/plasma partition coefficients and the models were calibrated and evaluated with pharmacokinetic data from Food Animal Residue Avoidance Databank (FARAD). Results showed that model predictions were, in general, within a 2-fold factor of experimental data for all 3 drugs in both species. Following extralabel administration and respective U.S. FDA-approved tolerances, predicted WDIs for both cattle and swine were close to or slightly longer than FDA-approved label withdrawal times (eg, predicted 8, 28, and 7 days vs labeled 4, 28, and 4 days for flunixin, florfenicol, and penicillin G in cattle, respectively). The final model was converted to a web-based interactive generic PBPK platform. This PBPK platform serves as a user-friendly quantitative tool for real-time predictions of WDIs for flunixin, florfenicol, and penicillin G following FDA-approved label or extralabel use in both cattle and swine, and provides a basis for extrapolating to other drugs and species.

**Key words:** drug residue; Food Animal Residue Avoidance Databank (FARAD); food safety; interactive generic physiologically based pharmacokinetic (igPBPK) model; withdrawal interval (WDI).

Drug residues that exceed allowable concentrations or unsafe chemical substances in animal-derived food products are a challenge to global food safety (Baynes et al., 2016; Canton et al., 2021; Vanselow and Griffith, 2001). Generally, veterinary drugs are used to prevent or treat infectious diseases, improve feed efficiency, and enhance productivity in food-producing animals (Cully, 2014). However, these benefits are associated with the risk of drug residues above regulatory safety levels resulting in human health hazards (Durso and Cook, 2014). Violative residues within edible products or tissues of treated animals could increase the health risk to consumers or even result in the suspension of the producer's permit or certification to affect the global food trade of the agricultural product (NRC, 1999). Violative residues can often be caused by inappropriate extralabel drug use and/or failure to observe an adequate withdrawal interval (WDI) (KuKanich et al., 2005). Therefore, in order to prevent drug residue violations and protect human food safety relative to consumption of animal-derived food products, it is important to develop a scientifically based approach to estimate tissue residues and WDIs of drugs in food-producing animals (Canton et al., 2021; Riviere et al., 2017).

A physiologically based pharmacokinetic (PBPK) model is a mechanism-based model that is capable of describing the absorption, distribution, metabolism, and excretion of chemicals in different species by incorporating physiological- and compound-specific parameters (Lin et al., 2016a). Over the past several decades, PBPK models have been widely used in many fields including animal-derived food safety assessment (Henri et al., 2017; Li et al., 2019a), nanomedicine (Lin et al., 2016b; Singh et al., 2020), as well as animal and human health risk assessment of environmental chemicals (Chou and Lin, 2020; Lautz et al., 2020; Lin et al., 2017; Tan et al., 2018). In particular, in the field of food safety, multiple PBPK models have been developed for several veterinary drugs in different food animals by multiple research groups from different countries to determine drug WDIs based on their respective regulatory standards (Henri et al., 2017; Riad et al., 2021; Yang et al., 2019; Zhou et al., 2021). Estimation of WDIs using a scientific tool such as PBPK models may be very useful to avoid violative drug residues and keep animal-derived food products safe for human consumption when drugs are used under field conditions.

The Food Animal Residue Avoidance Databank (FARAD) program is a U.S. Congressionally authorized U.S. Department of Agriculture-supported national food safety program with the mission of helping producers and veterinarians prevent or mitigate illegal or harmful residues of drugs, pesticides, biotoxins, and other chemical agents that may contaminate foods of animal origin (Riviere et al., 2017). To achieve this mission, FARAD researchers collect and analyze pharmacokinetic data in order to develop pharmacokinetic models, including PBPK models, to help answer requests from veterinarians for WDIs for drugs prescribed extralabel in food animals. Of note, every year FARAD receives thousands of WDI requests for many different drugs administered to various food animal species that directly impact millions of food animals as well as indirectly benefiting numerous consumers (internal data from FARAD Call Centers). However, existing PBPK models are either limited to 1 specific drug or difficult to use by individuals without programming experience. PBPK models are relatively complex in nature and

require numerous model parameters such as metabolic rates and tissue partition coefficients as input. Thus, it is not easy to adapt a model developed for 1 drug to use for other drugs, especially considering that different drugs often have different metabolic processes. Therefore, existing PBPK models are not sufficient to address the food safety concern and WDI requests for many drugs dosed with various therapeutic regimens in a timely manner. A user-friendly generic PBPK model platform that can be applied to multiple drugs is urgently needed to address this national and global food safety need.

Therefore, the objective of this study was to develop a web-based generic PBPK modeling platform that can be used to estimate tissue residues and WDIs of multiple drugs rapidly and easily in different food animal species. To develop and evaluate this modeling platform, we chose flunixin, florfenicol, and penicillin G as representative medications and selected cattle and swine as model species. These 3 drugs were selected as they are medications for which FARAD received the most WDI requests over the last several years (Li et al., 2017, 2019a; Yang et al., 2019). In addition, our research team previously developed PBPK models for each of these medications individually (Li et al., 2017, 2019a; Yang et al., 2019). These earlier studies provide a basis to develop the present more robust and comprehensive PBPK model and enable comparisons of simulation results between different models. In addition, new pharmacokinetic studies have been published since the development of these earlier models. In real-time residue mitigation events, it is ideal to incorporate new published datasets to improve existing PBPK models so that they are more robust than the originally developed model. Cattle and swine were selected as the model species because they are included in the FDA's list of major food animal species in the United States. In this study, a species-specific tissue composition-based *in silico* model was incorporated to estimate the tissue-to-plasma partition coefficients. As such, the final PBPK model is more flexible and may be extrapolated to other food animal species. To ensure user-friendliness, the final PBPK model was converted to a web-based interactive visualization platform.

## MATERIALS AND METHODS

**Pharmacokinetic data for model development.** All pharmacokinetic data used in model calibration and evaluation were acquired from the FARAD Comparative Pharmacokinetic Database (<http://www.farad.org>) (Riviere et al., 2017) with the keywords "Flunixin," "Florfenicol," and "Penicillin G." The pharmacokinetic data for cattle and swine following oral, intravenous (IV), intramuscular (IM), and subcutaneous (SC) administration were selected. Data in dairy cows and lactating sows were excluded because of the additional elimination route through milk that may result in differences in the pharmacokinetics between lactating and non-lactating animals. The pharmacokinetic datasets of flunixin, florfenicol, and penicillin G in plasma or tissues were collected from tables or digitized from figures in the literature using WebPlotDigitizer (version 4.4, <https://automeris.io/WebPlotDigitizer>). A summary of key information of selected pharmacokinetic studies is provided in Table 1.

**Table 1.** A Summary of Pharmacokinetic Studies Used for Model Calibration and Evaluation

Reference	Routes	Dose (mg/kg)	Repeat dose	Species	Matrix	Compounds	Use
<b>Flunixin</b>							
Howard et al. (2014)	IV	3	Single	Swine	P	FLU, 5OH-FLU	Cal
Pairis-Garcia et al. (2013)	IV, IM, PO	2.2	Single	Swine	P	FLU	Cal
FDA (2005)	IM	2.2	3 days	Swine	L, M, K, F	FLU	Cal
Buur et al. (2006)	IV	2	Single	Swine	P	FLU	Cal
EMA (1999)	IM	2.4	3 days	Swine	L, M, K	FLU	Cal
Bates et al. (2020)	IM	2.2	Single	Swine	P, L, K, M, U	FLU, 5OH-FLU	Cal
Kittrell et al. (2020)	IM, PO	2.2 (IM); 3.3 (PO)	Single	Swine	P	FLU	Eval
FDA (1998)	IV	2.2	3 days	Cattle	L, M, K, F	FLU	Cal
Shelver et al. (2013)	IV, SC	2.2	Single	Cattle	P	FLU, 5OH-FLU	Cal
Odensvik and Johansson (1995)	IV, IM	2.2	Single	Cattle	P	FLU	Cal
Kissell et al. (2016)	IV	2.2	3 days	Cattle	P, L, M, K	FLU, 5OH-FLU	Eval
Jaroszewski et al. (2008)	IV	2.2	4 days	Cattle	P	FLU, 5OH-FLU	Cal
Kleinhenz et al. (2016)	IV	2.2	Single	Cattle	P	FLU	Cal
Odensvik (1995)	IV	2.2	Single	Cattle	P	FLU	Cal
<b>Florfenicol</b>							
Embrechts et al. (2013)	IM	22.5, 30, 15	Single or 2 days	Swine	P	FLO	Cal
Jiang et al. (2006)	IV, IM, PO	20	Single	Swine	P	FLO	Cal
Kim et al. (2008)	IM	5, 20	Single	Swine	P	FLO	Cal
Li et al. (2002)	IM	20	Single	Swine	Lu, K, M, L, and P	FLO	Cal
Liu et al. (2003)	IV, IM, PO	20	Single	Swine	P	FLO	Cal
SPAHC (2002)	PO (water)	20	Single	Swine	L, K, M, and F	FLOA	Cal
SPAHC (2006)	PO	10	5 days	Swine	L, K, M, and F	FLOA	Eval
Voorspoels et al. (1999)	IM, PO	15, 15	Single, 3 days	Swine	P	FLO	Cal
Zhang et al. (2016)	IM	20	Single	Swine	P	FLO	Cal
Lei et al. (2018)	IM, IV	30	Single	Swine	P	FLO	Eval
Varma et al. (1986)	IV, PO	22	Single	Cattle	S	FLO	Cal
Sidhu et al. (2014)	SC	40	Single	Cattle	S	FLO	Cal
Lobell et al. (1994)	IV, IM	20	Single	Cattle	S	FLO	Cal
Lacroix et al. (2011)	IM, SC	40	Single	Cattle	P	FLO	Cal
Gilliam et al. (2008)	IV	2.2	Single	Cattle	S	FLO	Cal
de Craene et al. (1997)	IV	20	Single	Cattle	P	FLO	Cal
Croubels (2006)	PO	20	Single	Cattle	P	FLO	Cal
Bretzlaff et al. (1987)	IV	50	Single	Cattle	P	FLO	Cal
SPAHC (2008)	SC	40	Single	Cattle	L, K, M	FLOA	Cal
Norbrook Laboratories (2015)	SC	40	Single	Cattle	L, M	FLOA	Eval
Intervet Inc. (2009)	SC	40	Single	Cattle	L	FLOA	Cal
<b>Penicillin G</b>							
Ranheim et al. (2002)	IM, SC	99	Single	Swine	P	PG	Cal
Korsrud et al. (1998)	IM	14.9, 65.4	3, 5 days	Swine	L, K, M, F, and P	PG	Cal
Korsrud et al. (1998)	IM	14.9	3 days	Swine	K, M, and P	PG	Cal
Lupton et al. (2014)	IM	32.5	3 days	Swine	P, M, and K	PG	Eval
Li et al. (2019b)	IM	6.5, 32.5	3 days	Swine	P, M, L, and K	PG	Cal
Papich et al. (1993)	IM, SC	23.7, 65.4 (IM); 65.4 (SC)	5 days or single (IM), single (SC)	Cattle	P	PG	Cal
Korsrud et al. (1993)	IM	23.7, 65.4	5 days	Cattle	L, K, M, and P	PG	Cal
Trolldenier et al. (1986)	SC	8.9	Single	Cattle	P	PG	Cal
Chiesa et al. (2006)	IM	6.9	3 days	Cattle	K, P	PG	Eval
Djebala et al. (2021)	IM	20.8	Single	Cattle	P	PG	Cal

Only concentration data above limits of quantification in selected studies were used for model calibration or evaluation.

Abbreviations: Cal, Calibration; Eval, Evaluation; F, fat; FLU, flunixin; FLO, florfenicol; FLOA, florfenicol amine; K, kidneys; NA, not available or not applicable; L, liver; M, muscle; P, plasma; PO, oral; PG, penicillin G; and 5OH-FLU, 5-hydroxy flunixin.

**Model structure.** A generic PBPK model structure was designed for simulations of concentration versus time profiles for the 3 selected drugs. The model structure, based on previous PBPK models (Li et al., 2017, 2019a; Yang et al., 2019), was designed to include 2 submodels, which are capable of simulating the parent compounds: flunixin, florfenicol, and penicillin G, and their corresponding major metabolites (when applicable) (Figure 1). The major metabolites of flunixin and florfenicol, 5-hydroxy flunixin, and florfenicol amine, respectively, were specifically described in the metabolite submodel. Because the metabolism of penicillin G in food-producing animals is minimal, the liver metabolism of penicillin G was described by a simplified first-order model without monitoring the distribution of its specific metabolites in the model. The parent compound submodel was composed of major edible tissues including liver, kidney, muscle, fat (a.k.a. adipose tissue), and the rest of the body connected by a blood compartment representing circulating blood system (Figure 1). The administration routes of oral, IV, IM, and SC were incorporated into the parent drug submodel. IM and SC injections were described as 2-compartment injection site model (injection sites 1 and 2 were denoted as the fast absorption and slow releasing sites) with dissolution processes from site 2 to site 1 (Supplementary Equations 1–6) based on the previous studies (Lin et al., 2015, 2017; Yang et al., 2019). This approach divided the drug into dissolved moieties that are immediately available for absorption (fast) and undissolved drug acting as a depot that is released slowly (slow). Oral administration was described as a 2-compartment model consisting of stomach and intestines to simulate the absorption of drug in the stomach and then transportation to the intestinal tract via gastric emptying (Supplementary Equations 7–9). The same model structure without absorption routes and fat compartment was used in the metabolite submodel and connected with the parent drug model through hepatic metabolism. The elimination routes, including urine, biliary, and feces, were included in the parent drug submodel, while only urine and biliary excretion was considered in the metabolite submodel. Enterohepatic circulation was also considered in the model for all 3 drugs based on previous studies (Li et al., 2017; Lin et al., 2015; Yang et al., 2019). All the above-mentioned mathematical equations (Supplementary Equations 10–16) are described in detail in the Supplementary Data.

**Model parameterization.** Two different types of parameters were used in the generic PBPK model, including species-specific physiological parameters and chemical-specific parameters. The species-specific physiological parameters such as body weight (BW), cardiac output (QCC), fractions of blood flow to individual tissues (eg, the fraction of blood flow to liver, QLC) as well as the volume fractions of organs (eg, the volume fraction of liver, VLC) were collected from a recent comprehensive review article (Lin et al., 2020b) where these parameters were collected and summarized from published experimental data. All species-specific physiological parameters are summarized in Table 2. Chemical-specific parameters consisted of protein binding parameters, absorption rate constant, elimination rate constant, metabolic rate constant, and partition coefficients. Protein binding parameters were obtained from experimental studies in cattle and swine (Adams et al., 1987; Galbraith and McKellar, 1996; Peterson, 1978) or the fitting values from previous PBPK models (Buur et al., 2006; Li et al., 2017, 2019b; Yang et al., 2019). Absorption rate, metabolic rate, urinary, fecal, and biliary elimination rate constants were collected from previous PBPK models for the 3 selected medications (Li et al., 2017,

2019b; Yang et al., 2019). Tissue-to-plasma partition coefficient parameters were predicted using mechanism-based *in silico* models (further described below). These parameter values were used as initial values in the model calibration and optimized with measured pharmacokinetic data (Table 1). All collected and optimized chemical-specific parameters are provided in Table 3 for cattle and Table 4 for swine.

**Estimation of partition coefficients in cattle and swine.** In order to estimate tissue-to-plasma partition coefficients for drugs without experimentally measured values, a compiled integrative algorithm consisting of 5 frequently used mechanistic equations (Berezhkovskiy, 2004; Poulin and Theil, 2002; Rodgers et al., 2005; Rodgers and Rowland, 2006; Schmitt, 2008) was developed and incorporated into the PBPK model. The tissue composition data in cattle and swine (Aksu et al., 2017; Haritova and Fink-Gremmels, 2010; Poulin et al., 2019; Utsey et al., 2020) and physicochemical properties (eg, logP and pKa) for flunixin, florfenicol, and penicillin G were incorporated into the model to estimate the partition coefficients for each of the tissues in each species. Then the average predicted tissue-to-plasma partition coefficients from the 5 different models were used as initial values in the model calibration by fitting to available pharmacokinetic datasets. The detailed equations for all these methods (Supplementary Equations 17–21), tissue composition data in both cattle and swine (Supplementary Tables 1 and 2), and physicochemical properties of the 3 selected drugs (Supplementary Table 3) are provided in the Supplementary Data.

**Model calibration and evaluation.** Following model parameterization, the generic PBPK model was further calibrated with measured pharmacokinetic raw concentration data (ie, untransformed data) using the Levenberg-Marquardt least-squares algorithm (Chou and Lin, 2019) implemented in the R package FME. Briefly, the parameters  $\theta$  were calibrated by comparing the predicted values  $f(t_{ij}, \theta)$  with the mean measured values  $y_{ij}$  at time point  $i$  of the data set  $j$ . The least-squares function between the observed and simulated values was estimated as

$$\hat{\theta} = \operatorname{argmin}_{\theta} \sum_{ij} \left[ \frac{f(t_{ij}, \theta) - y_{ij}}{w_{ij} \times n_j} \right]^2, \quad (1)$$

where the  $w_{ij}$  is a weighting factor that normalizes the difference of units or magnitudes from a variety of data sources. The  $w_{ij}$  can be estimated from the standard deviation of measured values.  $n_j$  represents the number of data points for data set  $j$  which was used to scale the residuals to prevent abundant data set dominating the analysis. The model was fitted with pharmacokinetic data sets simultaneously and the optimized parameters  $\hat{\theta}$  were estimated when the minimum of sum of squared residuals for all data points from all data sets.

With the optimized parameter values, the evaluation of the PBPK model was conducted by comparing model simulations with independent pharmacokinetic data sets (ie, data not used in model calibration). On the basis of the PBPK modeling guidelines from World Health Organization (WHO, 2010) and Organization for Economic Co-operation and Development (OECD, 2021), the model was considered to be reasonable and acceptable when the simulation results matched the pharmacokinetic profiles and were generally within a 2-fold difference of observed values. The global evaluation of model fit between

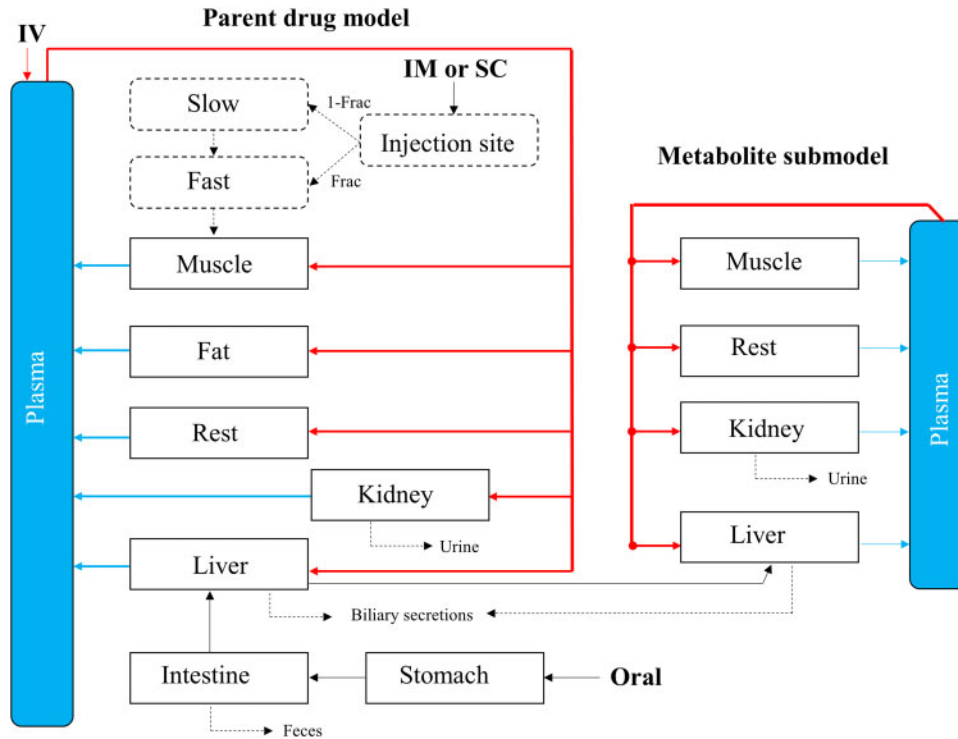


**Figure 1.** A schematic diagram of the generic PBPK model for flunixin, florfenicol, and penicillin G in cattle and swine. A metabolite submodel was included to account for the main metabolite when needed, such as 5-hydroxy flunixin for flunixin and florfenicol amine for florfenicol. Four different administration routes, including oral, IV, IM, and SC administrations are presented in the model. A 2-compartment absorption model (fast/slow) was used to describe the IM and SC injections. The parameter Frac is the fraction of the drug that is readily available for fast absorption (unitless) after IM or SC injection.

**Table 2.** Physiological Parameters Values Used in the Generic PBPK Model in Cattle and Swine

Parameter	Abbreviation	Cattle	Swine
Cardiac output (L/h/kg)	QCC	5.45 (1.47)	8.7 (1.62)
Hematocrit	Htc	0.378 (0.046)	0.412 (0.05)
Blood flow (fraction of cardiac output, unitless)			
Liver	QLC	0.44 (0.25)	0.273 (0.082)
Kidney	QKC	0.11 (0.08)	0.114 (0.032)
Muscle	QMC	0.28 (0.09)	0.342 (0.306)
Fat	QFC	0.08 (0.024)	0.128 (0.038)
Rest of body	QRestC	1-QLC-QKC-QMC-QFC	
Rest of body for metabolites	QRestC1	1-QLC-QKC-QMC	
Tissue volume (fraction of BW, unitless)			
Plasma	VPC	0.0399 (0.0068)	0.0412 (0.0046)
Liver	VLC	0.0122 (0.0018)	0.0204 (0.0033)
Kidney	VKC	0.0021(0.0005)	0.0037 (0.0011)
Muscle	VMC	0.361 (0.1173)	0.3632 (0.0266)
Fat	VFC	0.1218 (0.0506)	0.1544 (0.0265)
Rest of body	VRestC	1-VLC-VKC-VMC-VFC	
Rest of body for metabolites	VRestC1	1-VLC-VKC-VMC	

All parameter values in both cattle and swine were collected from [Lin et al. \(2020b\)](#), except QFC in cattle and swine and QLC in swine were collected from [Li et al. \(2017\)](#). The value was expressed as “mean (SD).”

log-transformed values of experimentally observed and model-predicted drug concentrations in plasma and tissues was further analyzed to determine the coefficient of determination ( $R^2$ ).

**Sensitivity analysis.** Sensitivity analysis can be used to identify sensitive parameters that have high impacts on the model outputs (eg, selected dose metrics). In this study, a local sensitivity analysis was performed to determine which parameters were

most influential on the 24-h area under curves (AUC) of liver, kidney, and muscle concentrations of flunixin, florfenicol, and penicillin G in cattle and swine following respective label use regimens. By increasing 1% of each parameter value and calculating the corresponding AUCs, normalized sensitivity coefficients (NSCs) were estimated to evaluate the relative sensitivity of each parameter on the corresponding AUC using the equation reported previously ([Chou and Lin, 2021](#); [Lin et al., 2013](#);

**Table 3.** Chemical-Specific Parameter Values Used in the PBPK Model for Flunixin, Florfenicol, and Penicillin G and in Cattle

Parameter	Symbol	Flunixin	Florfenicol	Penicillin G
Absorption rate constant (/h)				
IM administration	Kim	1 <sup>a</sup>	0.16 <sup>b</sup>	0.10*
	Fracim		0.71*	0.65*
	Kdissim		0.01 <sup>b</sup>	0.001*
SC administration	Ksc	0.4 <sup>a</sup>	0.12 <sup>b</sup>	0.04*
	Fracsc		0.56*	0.76*
	Kdissc		0.005*	0.005 <sup>c</sup>
Molecular weight				
Parent compounds		296.4 <sup>d</sup>	358.2 <sup>d</sup>	334 <sup>d</sup>
Metabolites		312.4 <sup>d</sup>	247.3 <sup>d</sup>	
Tissue-to-plasma partition coefficient for parent compound (unitless)				
Liver	PL	2.19*	1.98*	1.09*
Kidney	PK	3.38*	0.91*	1.98*
Muscle	PM	0.43*	1.33 <sup>e</sup>	0.20*
Fat	PF	0.56*	0.61*	0.04 <sup>c</sup>
Rest of body	PRest	6.74*	0.12*	7.99*
Tissue-to-plasma partition coefficient for parent metabolite (unitless)				
Liver	PL1	3.11 <sup>f</sup>	7.59*	
Kidney	PK1	4.59*	1.30 <sup>f</sup>	
Muscle	PM1	2.96 <sup>e</sup>	0.90 <sup>f</sup>	
Rest of body	PRest1	8.04*	0.09*	
Hepatic metabolic rate constant (/h/kg)	KmetC	0.005*	0.23*	0.25*
Rate constant for enterohepatic circulation (/h/kg)	KehcC	0.012*	0.13*	0.0004*
Free fraction of chemical in plasma (unitless)				
Parent compound	fR	0.15*	0.79*	0.66*
Metabolites	fR1	0.008*	0.71 <sup>b</sup>	
Biliary elimination rate (L/h/kg)				
Parent compound	KbileC	0.51*	0.11*	0.63*
Metabolites	KbileC1	0.58*	0.16*	
Urinary elimination rate constant (L/h/kg)				
Parent compound	KurineC	0.50*	0.32*	0.825*
Metabolites	KurineC1	0.068*	0.002*	
Intestinal absorption rate constant (/h)	Kabs	0.4 <sup>a</sup>	1.9 <sup>g</sup>	1.9 <sup>g</sup>
Fecal elimination rate constant (/h)	Kunabs	0.81*	0.009*	0.51*

<sup>a</sup>Li et al. (2019a).<sup>b</sup>Yang et al. (2019).<sup>c</sup>Li et al. (2017).<sup>d</sup>PubChem.<sup>e</sup>Assumed to be equal to the value of parent compounds<sup>f</sup>Predicted value by using an *in silico* model (described in the Materials and Methods section)<sup>g</sup>Assumed same as the value of florfenicol model from the previous study (Yang et al., 2019).

\*The parameter values in bold were obtained through model fitting. Regarding the model fitting, refer to the Materials and Methods section for further information on which datasets were used to estimate values for these parameters.

Mirfazaelian et al., 2006). The detailed equation is provided in the Supplementary Data (Supplementary Equation 22).

**Establishment of a population PBPK model.** Monte Carlo simulations were incorporated into the generic PBPK model to obtain population-based simulations based on repeated random sampling from the designated distribution of each parameter. Each Monte Carlo simulation contained 1000 iterations (ie, 1000 animals). For these simulations, all physiological and chemical-specific parameters were randomly sampled around mean values of the specified distributions, and their variability was defined by coefficients of variance (CVs). Based on the default assumptions reported in previous PBPK modeling studies (Henri et al., 2017; Li et al., 2017; Yang et al., 2015), log-normal distributions were assumed for all chemical-specific parameters, and

the physiological parameters (except blood flow fractions) were assumed to follow normal distributions. Due to the high variability of blood flow fractions in cattle and swine collected from experimental data (Lin et al., 2020b), the log-normal distribution was used to avoid producing negative values. CV values for most of the physiological parameters including the BW, cardiac output, and tissue volume fractions of liver and kidneys, and the fractions of blood flows in liver were calculated based on the experimental data from a comprehensive review article (Lin et al., 2020b). For the other physiological parameters whose CV values were unknown, a default CV of 30% was used. For chemical-specific parameters, based on previous studies, a CV of 20% was assigned to tissue-to-plasma partition coefficients (Henri et al., 2017; Li et al., 2017; Yang et al., 2015), 30% for absorption, metabolic, and elimination rate constants (Li et al., 2018;

**Table 4.** Chemical-Specific Parameter Values Used in the PBPK Model for Flunixin, Florfenicol, and Penicillin G and in Swine

Parameter	Symbol	Flunixin	Florfenicol	Penicillin G
Absorption rate constant (/h)				
IM administration	Kim	1 <sup>a</sup>	0.21*	0.10*
	Fracim		0.56*	0.55*
	Kdissim		0.0253*	0.007 <sup>b</sup>
SC administration	Ksc	0.4 <sup>a</sup>	0.128 <sup>c</sup>	0.25 <sup>b</sup>
	Fracsc		0.50 <sup>c</sup>	0.5 <sup>b</sup>
	Kdisssc		0.005 <sup>c</sup>	0.005 <sup>b</sup>
Tissue-to-plasma partition coefficient for parent compound (unitless)				
Liver	PL	2.30*	0.39*	0.07*
Kidney	PK	6.99*	3.47 <sup>d</sup>	1.43*
Muscle	PM	0.31*	1.3 <sup>d</sup>	0.08*
Fat	PF	0.6 <sup>d</sup>	0.15*	0.25 <sup>d</sup>
Rest of body	PRest	20.7*	1.16*	0.46*
Tissue-to-plasma partition coefficient for parent metabolite (unitless)				
Liver	PL1		14.7*	
Kidney	PK1		5.98*	
Muscle	PM1		1.21*	
Rest of body	PRrest1		0.49*	
Hepatic metabolic rate constant (/h/kg)	KmetC	0.004*	0.0075*	0.59*
Rate constant for enterohepatic circulation (/h/kg)	KehcC	0.004*	0.17*	0.01*
Free fraction of chemical in plasma (unitless)				
Parent compound	fR	0.13*	0.59*	0.96*
Metabolites	fR1		0.78*	
Biliary elimination rate (L/h/kg)				
Parent compound	KbileC	0.401*	0.03*	0.52*
Metabolites	KbileC1	0.034*	5.98E-4*	
Urinary elimination rate constant (L/h/kg)				
Parent compound	KurineC	0.253*	0.43*	1.54*
Metabolites	KurineC1	0.007*	0.01*	
Intestinal absorption rate constant (/h)	Kabs	0.4 <sup>a</sup>	1.9 <sup>c</sup>	1.9 <sup>e</sup>
Fecal elimination rate constant (/h)	Kunabs	0.5 <sup>a</sup>	0.11*	0.81*

<sup>a</sup>Li et al. (2019a).<sup>b</sup>Li et al. (2017).<sup>c</sup>Yang et al. (2019).<sup>d</sup>Predicted value by using the in silico model (described in Materials and Methods section).<sup>e</sup>Assumed same as the value of florfenicol model from the previous study (Yang et al., 2019).<sup>\*</sup>The parameter values in bold were obtained through model fitting. Regarding the model fitting, refer to the Materials and Methods section for further information on which datasets were used to estimate values for these parameters.

Yang et al., 2015; Zeng et al., 2019), and 10% for protein binding constants (Li et al., 2017; Riad et al., 2021). Note that previous studies have shown that the CV values for plasma protein binding percentages of selected drugs were generally within 10% (Adams et al., 1987; Galbraith and McKellar, 1996; Peterson, 1978), so the use of the default CV value of 10% was conservative enough. The 2.5th and 97.5th percentiles of each parameter were calculated as the upper and lower bounds to ensure the values were biologically plausible for each of parameters. In addition, all physiological parameters were adjusted to ensure that the sum of tissue volumes or the sum of fractions of blood flows were equal to 1 after random sampling from defined distributions to avoid unbalance of the PBPK model.

*Estimation of WDIs using the population PBPK model.* The population PBPK model was used to account for population variability and parameter uncertainty and to generate population simulation results of flunixin, florfenicol, and penicillin G concentrations in plasma and edible tissues in diverse populations of cattle and swine following label or extralabel dosing regimens

in order to calculate WDIs. In this manuscript, FDA-approved withdrawal time (a.k.a. FDA-approved withdrawal period) refers to the time needed after label administration of a drug for tissue residue concentrations to decrease below tolerances determined using the 99th percentile tolerance limit method with a 95% confidence based on FDA guidance (FDA, 2018); whereas the term WDI is used to refer to the time for tissue residue concentrations to fall below tolerances estimated using other methods, such as the present population PBPK models and it is typically used when a drug is given in an extralabel manner. PBPK model-predicted WDIs in edible tissues were determined to be the time when the 99th percentiles of the simulated drug concentrations in target tissues fell below the tolerance in the United States or maximum residue limit from the European Medicines Agency of the drug in the corresponding tissue. For penicillin G, the tolerance for all edible tissues in cattle is 0.05 ppm or µg/g. The tolerance of penicillin G in swine is zero, so the minimum level of applicability of 0.025 µg/g (25 ng/g) from the USDA Food Safety and Inspection Services (USDA, 2013) was used for all edible tissues in swine. The tolerance of

flunixin in cattle is 0.125  $\mu\text{g/g}$  for liver and 0.025  $\mu\text{g/g}$  for muscle (FDA, 1998), and in swine is 0.03  $\mu\text{g/g}$  for liver and 0.025  $\mu\text{g/g}$  for muscle (FDA, 2005). Because there is no tolerance for flunixin in kidney for both cattle and swine, the tolerances for liver were used as a surrogate. The marker residue of florfenicol is the main metabolite florfenicol amine and the tolerance for florfenicol amine is 3.7  $\mu\text{g/g}$  for liver and 0.3  $\mu\text{g/g}$  for muscle in cattle, and 2.5 and 0.2  $\mu\text{g/g}$  for liver and muscle in swine, respectively (FDA, 2020). The tolerances of florfenicol amine in liver were used for kidney due to lack of published tolerances in kidney of cattle and swine.

*Development of an interactive generic PBPK model web interface.* An ordinary differential equation solver R package “mrgsolve” (Baron and Gastonguay, 2015) was used to solve the differential equations in the PBPK model code and was used in the final individual and population generic PBPK model. Then, the final generic PBPK model was converted to a web-based interactive generic PBPK (igPBPK) interface with the “Shiny” package in R program based on our recently published methods (Li et al., 2019b; Lin et al., 2020a; Riad et al., 2021).

*Code availability and result reproducibility.* All raw data that were used to calibrate and evaluate the present PBPK model and all model code, including the code files for the igPBPK web interface, the code files that were used to generate the results presented in figures, and the code files that were used to estimate tissue/plasma partition coefficients, as well as other relevant model code files along with additional instructions are available in the GitHub (<https://github.com/UFPBPK/FARAD-igPBPK>). These raw data and source code files will allow readers to reproduce our results and apply our model for further research.

## RESULTS

### Model Calibration and Evaluation

The generic PBPK model (Figure 1) was calibrated with concentrations of the 3 selected drugs and their metabolites in plasma and edible tissues following different exposure regimens corresponding to previous pharmacokinetic studies (Table 1). A global evaluation of goodness of fit was performed by comparison between model predictions and observed values for each drug (Figures 2A–C) and evaluating predicted-to-observed (P/O) ratio versus model prediction plots (Figures 2D–F), respectively. The model adequately simulated the calibration and evaluation datasets with the ranges of estimated coefficient of determination ( $R^2$ ) of 0.77–0.80 for flunixin and 5-hydroxy flunixin, 0.72–0.77 for florfenicol and florfenicol amine, and 0.78–0.80 for penicillin G (Figures 2A–C). The percentage of the predictions within 2-fold errors was 51.3%, 68.1%, and 57.3% for flunixin and 5-hydroxy flunixin (Figure 2D), florfenicol and florfenicol amine (Figure 2E), and penicillin G (Figure 2F) in cattle and swine, respectively. The range of the percentages within 3-fold errors was 71.7%–85.2% (Figures 2D–F). These results showed that more than 50% and 70% of model predictions were within a 2-fold and 3-fold factor of measured data, respectively.

Simulated results from the calibrated PBPK model were compared with measured concentrations from individual published studies in cattle and swine administered flunixin, florfenicol, or penicillin G through oral, IV, IM, or SC routes (representative results shown in Figure 3 for penicillin G and other results are shown in Supplementary Figures 1 and 2). The time-course comparisons for penicillin G in swine and cattle for the

calibration data (Figures 3A1–C3 for swine and Figures 3D5–F6 for cattle) showed that the model generally matched the kinetic profiles of penicillin G in plasma and edible tissues in both species. In addition, as shown in Figures 3C4–D4 and Figures 3H1 and 3H2 for evaluation data, model simulations for plasma, liver, kidney, and muscle of penicillin G were in agreement with most of the datasets. Overall, results from both analyses suggest that the model adequately simulates the observed data sets used for model calibration and evaluation.

### Sensitivity Analysis

Thirty-eight parameters were included in the local sensitivity analysis based on the dose metrics of 24-h AUCs of liver, kidney, and muscle concentrations of flunixin, 5-hydroxy flunixin, florfenicol, florfenicol amine, and penicillin G in cattle and swine following FDA-approved label use administration (Figure 4 and Supplementary Tables 4–7). Figure 4 is a representative figure displaying the absolute percentage of NSCs based on 24-h AUCs for muscle concentrations of flunixin, florfenicol, and penicillin G in cattle (Figure 4A) and swine (Figure 4B). The complete sensitivity analysis results for all edible tissues (eg, liver, kidney, and muscle) and all drugs with their metabolites (flunixin, 5-hydroxy flunixin, florfenicol, florfenicol amine, and penicillin G) can be found in Supplementary Tables 4–7. The results showed that the AUCs of the muscle for flunixin was highly sensitive to partition coefficient of muscle (PM), biliary excretion rate constant (KbileC), and fraction of blood flow to kidney (QKC) in both cattle (Figure 4A) and swine (Figure 4B). Similar high impacts on the AUCs of penicillin G were observed for the parameters of PM and the fraction of penicillin G immediately available for absorption (Fracim) via IM injection in both cattle and swine. The fraction of florfenicol immediately available for absorption (Fracim) via IM injection, urine elimination rate constant (KurineC), and PM was highly sensitive in the cattle model (Figure 4A), while the percentage of free drug (fR), cardiac output (QCC), blood flow of the kidney (QKC), KurineC, and PM was sensitive in the swine model (Figure 4B). For cattle, the QKC, VRestC (volume fraction of rest of body), and KurineC were the common sensitive parameters on AUCs of the selected tissues across flunixin, 5-hydroxy flunixin, florfenicol, florfenicol amine, and penicillin G (Supplementary Tables 4 and 6). In the swine model, the QKC and KurineC both were sensitive parameters on AUCs of all edible tissues for all drugs (Supplementary Tables 5 and 7). In addition, the partition coefficients of liver, kidney, and muscle were highly sensitive parameters (NSC > 0.5) on the prediction of AUCs in respective tissues for either cattle or swine model (Supplementary Tables 4–7).

### Monte Carlo Simulation and WDI Estimation

The population PBPK model coupled with the Monte Carlo sampling technique was used to estimate WDIs for flunixin, florfenicol, and penicillin G (Figures 5 and 6 and Table 5). All physiological and chemical-specific parameters were involved in the population analysis. Based on the simulation after FDA-approved label use in cattle (Figure 5), the concentrations of flunixin and florfenicol amine via IM injection depleted the slowest in muscle (Figures 5C and 5F), while the penicillin G concentration was decreased the slowest in liver (Figure 5G). For swine (Figure 6), the flunixin and penicillin G concentrations depleted the slowest in the kidney (Figures 6B and 6H), and the florfenicol amine concentration was decreased the slowest in the muscle (Figure 6F). The longest WDIs among tissues for



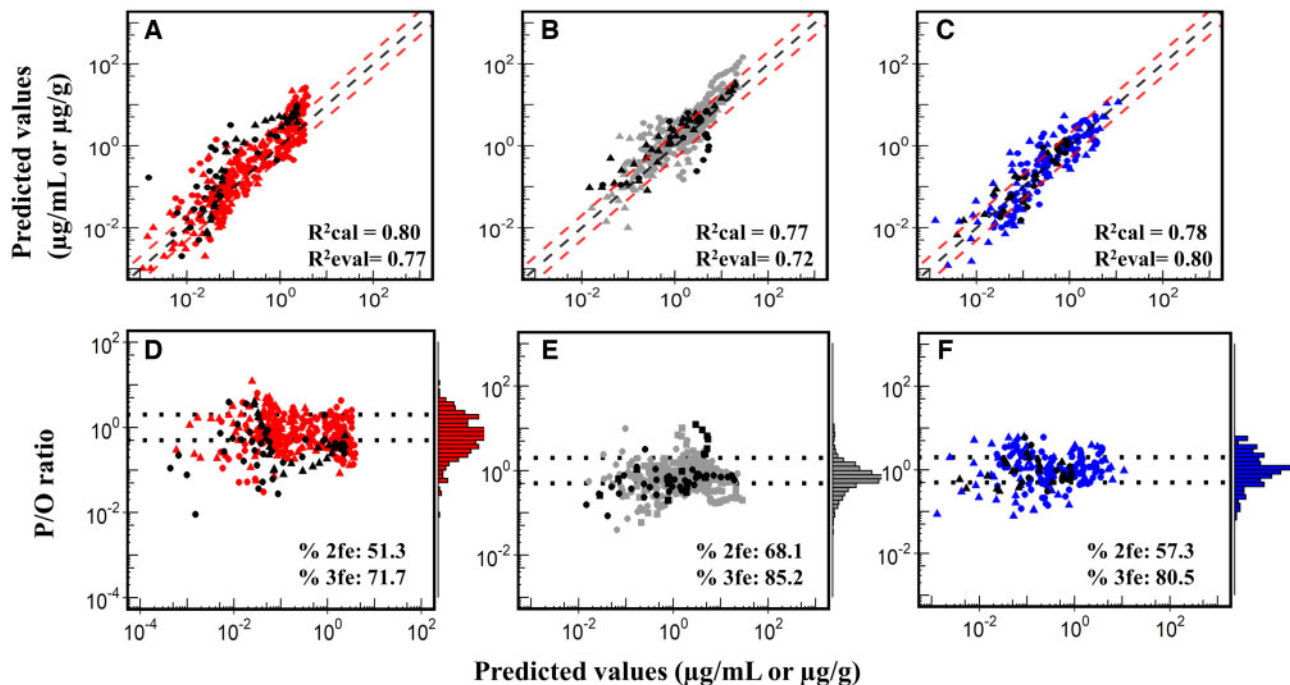


**Figure 2.** Model calibration and evaluation results. A global evaluation of goodness of model fit between the observed data (y-axis) and the model-predicted (x-axis) and P/O ratio versus model prediction plot for flunixin and 5-hydroxy flunixin (A, D), florfenicol and florfenicol amine (B, E), and penicillin G (C, F) in cattle and swine. Panels A–C represent goodness of model fit results. Panels D–F represent P/O ratio results. The dashed black diagonal line represents the unity line. The red dashed line represents 2-fold errors. Circle and triangle dots represent cattle and swine, respectively. The black dots represent the observed data from the model evaluation dataset. The red dots (A, D), gray dots (B, E), and blue dots (C, F) represent the observed data from the model calibration dataset. The abbreviations, %2fe and %3fe, represent the percentage of data points within 2-fold and 3-fold errors, respectively;  $R^2_{cal}$  and  $R^2_{eval}$  represent the determination coefficients estimated based on calibration data and evaluation data sets, respectively.

flunixin, florfenicol (after IM), florfenicol (after SC), and penicillin G in cattle and swine after FDA-approved label or extralabel dosing regimens were chosen to be the model-derived WDIs to compare with withdrawal times approved by regulatory agencies (Table 5).

The FDA-approved label dose regimens were obtained from the Veterinarian's Guide to Residue Avoidance Management (VetGRAM) (Riviere et al., 2017) and are listed in Supplementary Table 8. The estimated WDIs for flunixin, florfenicol (after IM), florfenicol (after SC), and penicillin G following FDA-label approved dosing regimens were 8 (muscle), 28 (muscle), 39 (muscle), and 7 (liver) days in cattle, respectively, while they were 14 (kidney), 16 (muscle), and 11 (kidney) days for flunixin, florfenicol, and penicillin G in swine (Figures 5 and 6 and Table 5). The predicted WDI following FDA-approved label dosing regimens in cattle were equal or close to FDA-approved label withdrawal times for florfenicol after IM administration (predicted WDI: 28 vs FDA-approved label withdrawal time: 28 days) and florfenicol after SC administration (predicted WDI: 39 vs FDA-approved label withdrawal time: 38 days), but were relatively longer for flunixin (predicted WDI: 8 vs FDA-approved withdrawal time: 4 days) and penicillin G (predicted WDI: 7 vs FDA-approved withdrawal time: 4 days). For swine, the predicted WDIs with FDA-approved label dosing regimens were both close to the FDA-approved label withdrawal times for flunixin (predicted WDI: 14 vs FDA-approved withdrawal time: 12 days), florfenicol (predicted WDI: 16 vs FDA-approved withdrawal time: 16 days), but were somewhat longer for penicillin G (predicted WDI: 11 vs FDA-approved withdrawal time: 6 days). From a food safety perspective, estimating longer WDIs is appropriate to minimize exposure to violative residues.

The extralabel dosing regimens for the 3 selected drugs were based on the internal WDI request data from 2019 to 2021 from FARAD Regional Call Centers, and are listed in Supplementary Table 9. Following these common extralabel dosing regimens for cattle and swine, the predicted WDIs in cattle were 8 (muscle), 29 (muscle), 48 (muscle), and 43 (liver) days for flunixin, florfenicol (after IM), florfenicol (after SC), and penicillin G (Table 5). For swine, the predicted WDIs were 22 (kidney), 22 (muscle), and 25 days (kidney), respectively (Table 5). The model-predicted WDIs in cattle and swine following extralabel dosing regimens were longer than FDA-approved label withdrawal times for all drugs (Table 5).

### User-Friendly Interface Establishment

The final generic PBPK model was converted into a web-based interactive igPBPK platform using the R Shiny package in R language and published online at the link: <http://pbpk.shinyapps.io/igPBPKApp>. A screenshot of this interface is shown in Figure 7. Users can input parameter values for each therapeutic regimen (eg, administration route, dosage, number of doses, and dosing interval) to the igPBPK interface to predict the concentrations of flunixin, florfenicol, and penicillin G and/or their metabolites in edible tissues. The interface will generate a detailed report of the simulation results and the predicted WDI based on the tolerance of the drug in a particular species and based on the simulated drug concentrations in the tissues for the defined therapeutic regimen. The results will be generated in real time (ie, a few seconds). A detailed tutorial on how to launch and use this igPBPK interface is provided in the Supplementary Data file.

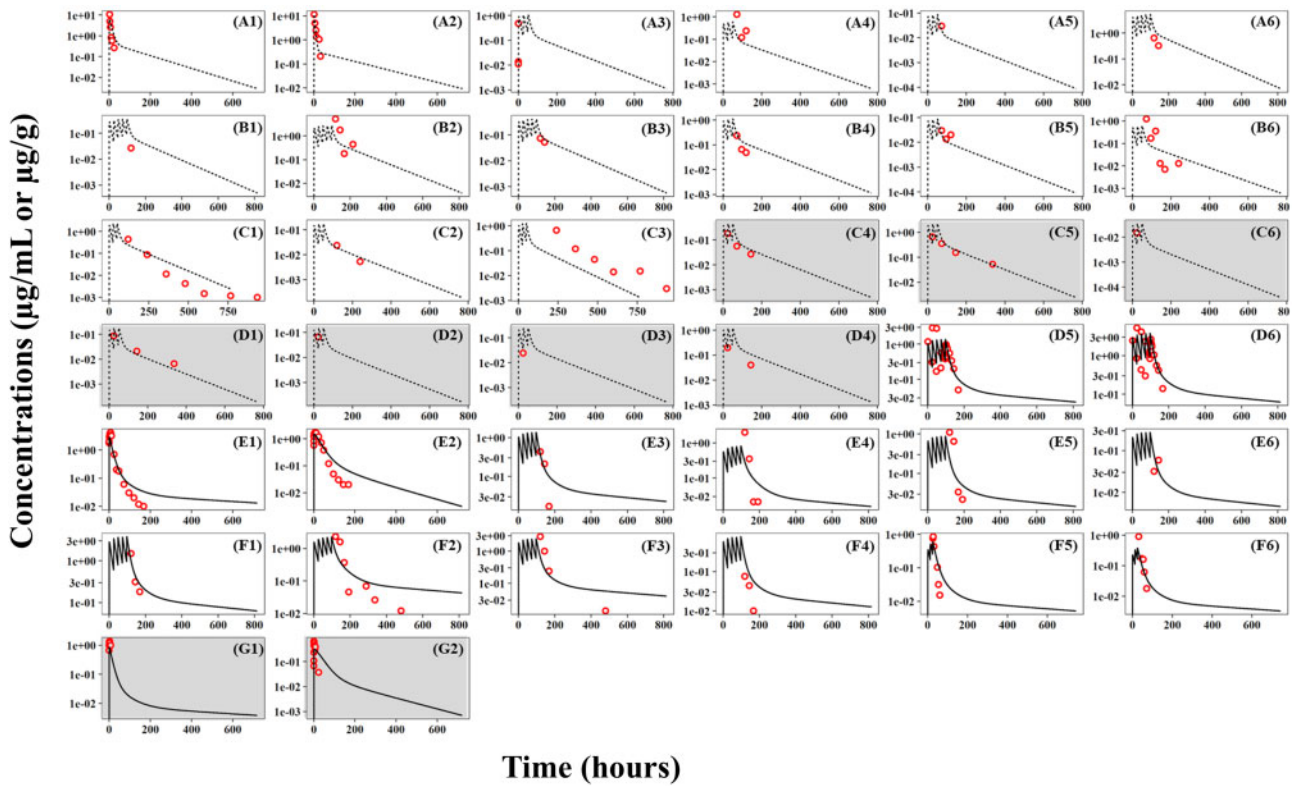


Figure 3. Model calibration and evaluation results of the PBPK model for penicillin G in swine (dashed line) and cattle (solid line). Comparisons of model prediction (lines) and observed data (red circles) are shown for concentrations of penicillin G in the plasma, liver, kidney, and muscle from swine and cattle. The plot with gray shadow represents the model evaluation results. Experimental data are from the studies of (A1–A2) (Ranheim et al., 2002), (A3–B3) (Korsrud et al., 1998), (B4–B6) (Lupton et al., 2014), (C1–C3) (Li et al., 2019b), (C4–D4) (Papich et al., 1993), (D5–E2) (Korsrud et al., 1993), (E3–F4) (Trolldenier et al., 1986), (F5) (Chiesa et al., 2006), and (F6–G2) (Djebala et al., 2021). Plots (D2), (C2, C6, and D1), and (C3, D3–D4, and G1) represent the liver, kidney, and muscle tissues, respectively, and other plots represent the plasma. Refer to Table 1 for the detailed dosing regimens from respective studies.

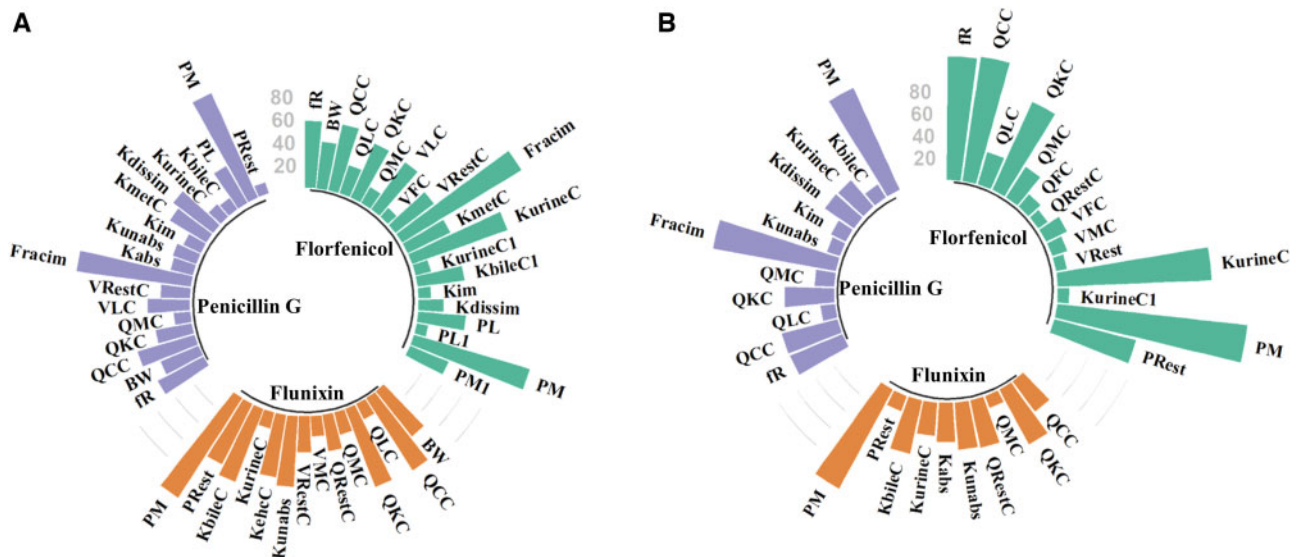
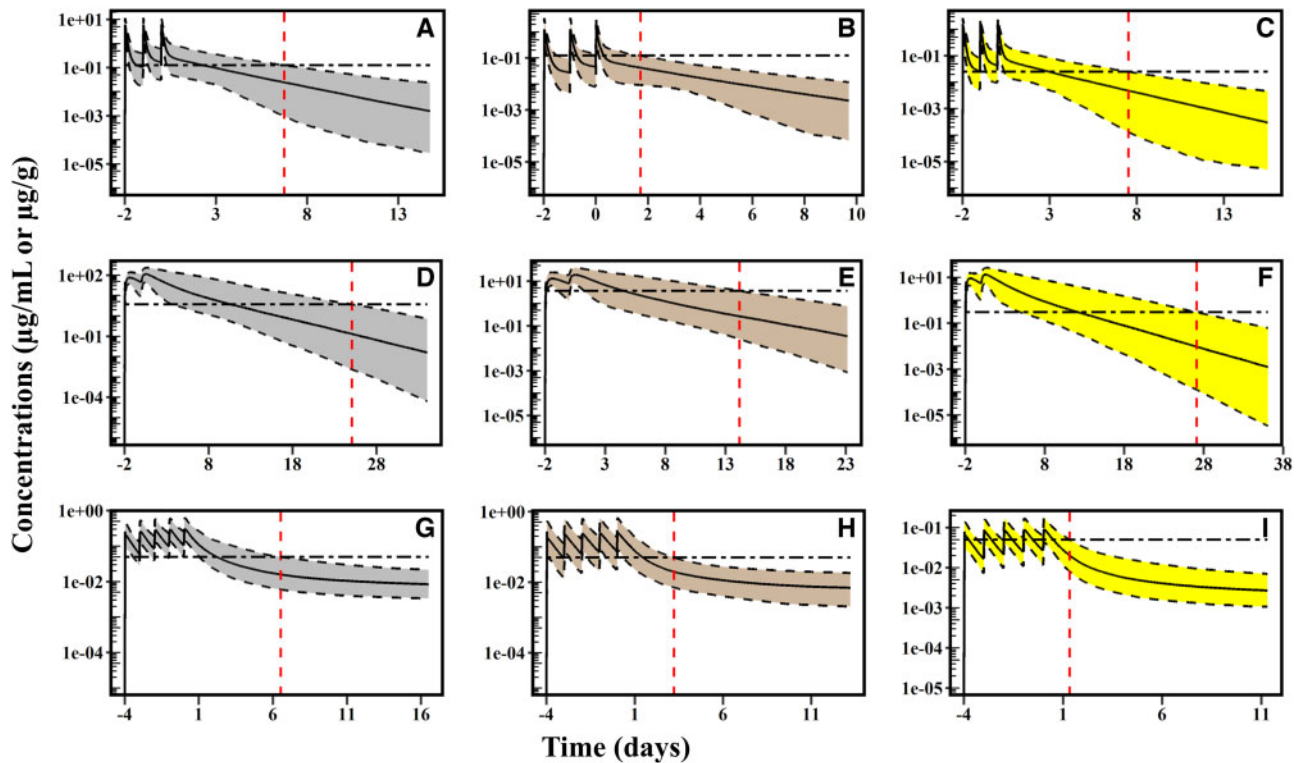


Figure 4. Sensitivity analysis results. The absolute percentages of NSCs of 24-h AUCs for concentrations of flunixin, florfenicol, and penicillin G in muscle in cattle (A) and swine (B). Only parameters with at least 1 absolute percentage of the NSC > 10% are shown on the plots. Refer to Tables 2–4 for definitions of parameters.

## DISCUSSION

This study reports a new igPBPK modeling web interface that can be used to simulate tissue residues and estimate WDIs of drugs with diverse physicochemical and pharmacokinetic

properties following different routes of administration (oral, IV, IM, and SC) in cattle and swine. Another novelty of this igPBPK interface is that all partition coefficients were estimated using *in silico* mechanistic equations. The strengths of this approach are that these parameters do not rely on animal tissue data to



**Figure 5.** Monte Carlo simulation results in cattle. Model-predicted concentrations of flunixin (A–C), florfenicol (D–F), and penicillin G (G–I) in liver (A, D, G), kidney (B, E, H), and muscle (C, F, I) for cattle following labeled dosing regimens (ie, flunixin: 2.2 mg/kg of 3 repeated IM injections with 24-h intervals; florfenicol: 20 mg/kg of 2 repeated IM injections with 48-h intervals; penicillin G: 6.5 mg/kg of 5 repeated IM injections with 24-h intervals). Each of the Monte Carlo simulations was run for 1000 iterations. The median (black solid line), 1th, and 99th (black dashed lines) percentiles of simulated results were plotted. The tolerance is shown on each of panels using a horizontal dashed line. The intersection between the x-axis and the black vertical line indicates the model-predicted WDIs. Refer to [Supplementary Table 8](#) for the details about tolerances of different drugs in different tissues in both species.

estimate their values and these mechanistic equations can be applied to other drugs. By integrating Monte Carlo simulations into the framework, the igPBPK model platform can generate health protective population-based simulation results to estimate WDIs for the 3 selected drugs following different exposure paradigms (both FDA-approved label and extralabel uses). This igPBPK interface serves as a useful tool to answer extralabel WDI inquiries in order to help ensure safety of animal-derived food products. This igPBPK model platform can be extended to other drugs in other species to help address food safety issues for the United States and other countries.

Several PBPK models for specific veterinary drugs (eg, florfenicol, monensin, penicillin G, and oxytetracycline) have been developed in recent years and used as a tool to facilitate drug WDI estimations ([Henri et al., 2017](#); [Law, 1999](#); [Li et al., 2019a, 2019b](#); [Riad et al., 2021](#); [Yang et al., 2019](#); [Zhou et al., 2021](#)). Some of these existing models have been converted to web-based user-friendly interactive PBPK interfaces, such as oxytetracycline ([Riad et al., 2021](#)) and flunixin ([Li et al., 2019a](#)). However, existing food animal PBPK models are typically limited to 1 specific drug for 1 model, and it requires extensive data, including tissue residue depletion data to adapt each model for each drug. This approach is time- and resource-intensive and it is an impossible task to develop a new model for each of the veterinary drugs in each species because there are so many drugs in different food animal species. Additionally, when new data become available, it is difficult to formulate new models. In this study, we developed an igPBPK platform that allows users without any modeling experience to quickly implement PBPK models. By

incorporating tissue-composition-based mechanistic equations into the model, the critical model parameters (ie, partition coefficients) can be predicted based on the physicochemical properties of the drug and based on the physiology of the animal. This is particularly important for drugs with limited data as it no longer requires tissue residue depletion data to estimate partition coefficients. This makes it possible to develop PBPK models for drugs with sparse data, with ready extrapolation to other drugs. In addition, compared with previous PBPK models for the 3 selected drugs, the present model is more robust as it was adapted and evaluated with additional new pharmacokinetic datasets ([Bates et al., 2020](#); [Djebala et al., 2021](#); [Kittrell et al., 2020](#); [Li et al., 2019b](#)). We expect that the concept of an interactive generic PBPK model platform will accelerate the development of the next generation of PBPK models in food animals to predict tissue residues and WDIs of animal drugs, including drugs with minimal pharmacokinetic data.

The present population PBPK model can be used to estimate WDIs based on FDA-approved label and extralabel use scenarios for the 3 selected drugs in cattle and swine. Model-predicted WDI for the 3 selected drugs in cattle and swine at the FDA-approved label doses, based on respective tolerances, is close to or equal to FDA-approved label withdrawal times ([Table 5](#)). For the common extralabel use of flunixin in cattle and swine (ie, 3 repeated IM injections at the dosage of 2.2 mg/kg with a 24-h dosing interval), the predicted WDI in cattle (8 days) is 4 days more than the FDA-approved withdrawal time (4 days for 3 repeated IV injections at a dosage of 2.2 mg/kg with a 24-h dosing interval), while the predicted WDIs in swine (22 days) is much

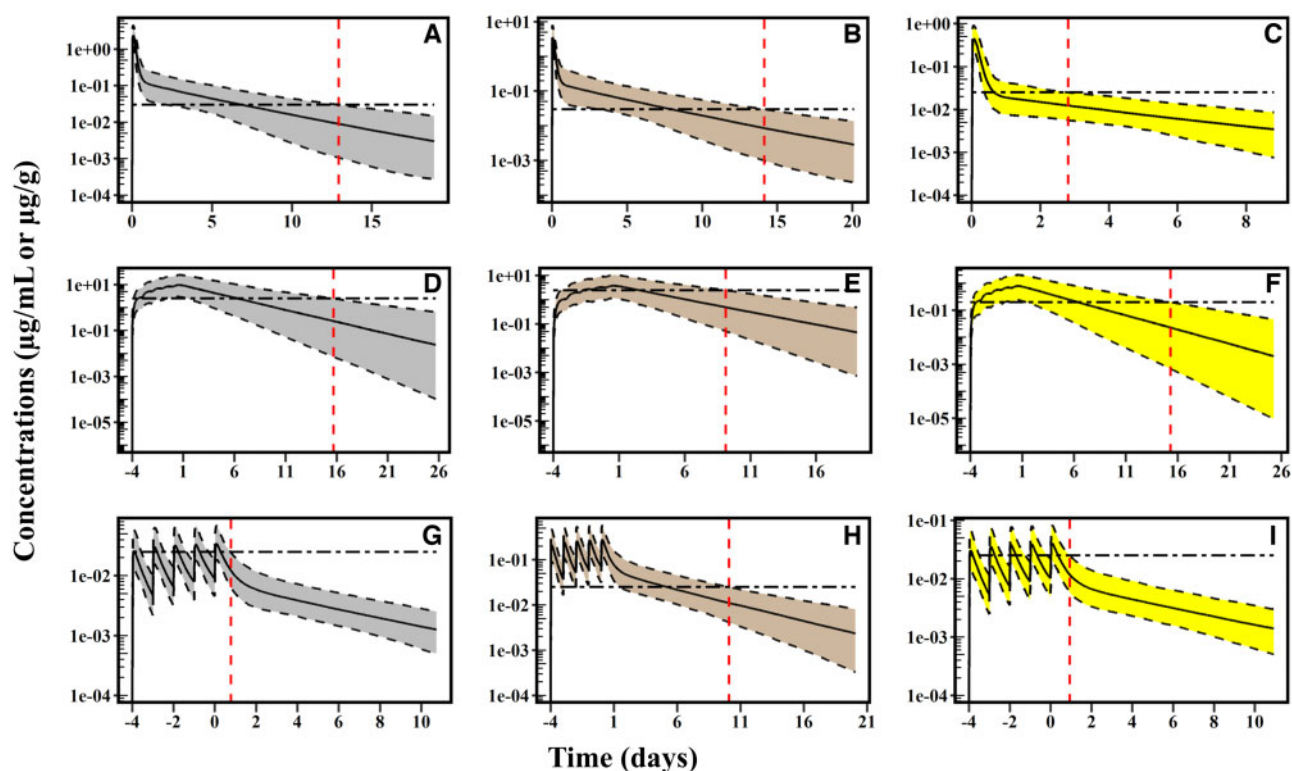


**Figure 6.** Monte Carlo simulation results in swine. Model-predicted concentrations of flunixin (A–C), florfenicol (D–F), and penicillin G (G–I) concentrations in liver (A, D, G), kidney (B, E, H), and muscle (C, F, I) for swine following labeled dosing regimens (flunixin: 2.2 mg/kg of a single IM injection; florfenicol: drinking water exposure at 100 ppm for 5 days equivalent to 14 mg/kg/day by oral exposure with 24-h intervals; penicillin G: 6.5 mg/kg of 5 repeated IM injections with 24-h intervals). Each of the simulations was run for 1000 iterations. The median (black solid line), 1th, and 99th (black dashed lines) percentiles of simulated results were plotted. The tolerance is shown on each of panels using the horizontal dashed line. The intersection between the x-axis and the black vertical line indicates the WDIs. Refer to [Supplementary Table 8](#) for the details about tolerances of different drugs in different tissues in both species.

**Table 5.** Comparisons of the Estimated WDIs for Flunixin, Florfenicol, and Penicillin G in Cattle and Swine with Labeled Withdrawal Times

Drugs	Calculated labeled WDIs based on the maximum residue limit or tolerance <sup>a</sup>			Calculated extralabeled WDIs based on the maximum residue limit or tolerance <sup>a</sup>			Labeled withdrawal times <sup>b</sup>
	Liver	Kidney	Muscle	Liver	Kidney	Muscle	
<b>Cattle</b>							
Flunixin	7	2	8	8	2	8	4
Florfenicol (IM) <sup>c</sup>	26	15	28	27	16	29	28
Florfenicol (SC) <sup>c</sup>	35	19	39	43	25	48	38
Penicillin G	7	3	2	43	34	8	4
<b>Swine</b>							
Flunixin	13	14	4	22	22	8	12
Florfenicol	16	10	16	22	12	22	16
Penicillin G	1	11	1	7	25	8	6

<sup>a</sup>For the label and extralabel dosing regimens, tolerance, and maximum residue limit, refer to [Supplementary Tables 8 and 9](#) for further information.

<sup>b</sup>The label withdrawal times were obtained from the VetGRAM of FARAD ([Riviere et al., 2017](#)).

<sup>c</sup>Florfenicol (IM) and Florfenicol (SC) indicate the simulations were based on the label and extralabel dosing scenarios via IM and SC administration, respectively. In this case of florfenicol, the main metabolite florfenicol amine was used as the marker residue.

longer than the FDA-approved withdrawal time (12 days for a single IM injection at a dosage of 2.2 mg/kg). The predicted WDIs for penicillin G in cattle and swine models following extralabel use [43 days (5 × label dose) in cattle and 25 days (5 × label dose) in swine] are both much longer than FDA-approved label withdrawal times (4 days for cattle and 6 days for swine). The results indicate that the predicted WDIs for the extralabel doses from the current model are more conservative, and thus more

protective, than withdrawal times that are based on the label dose. These results highlight the importance to use a scientific-based tool to estimate WDIs for different extralabel uses in order to avoid violative tissue residues of drugs in edible tissues of food animals.

Compared with the previous penicillin G and flunixin PBPK models ([Halleran et al., 2022](#); [Li et al., 2017, 2019a, 2019b](#)), when based on the label use, the predicted WDIs from the current

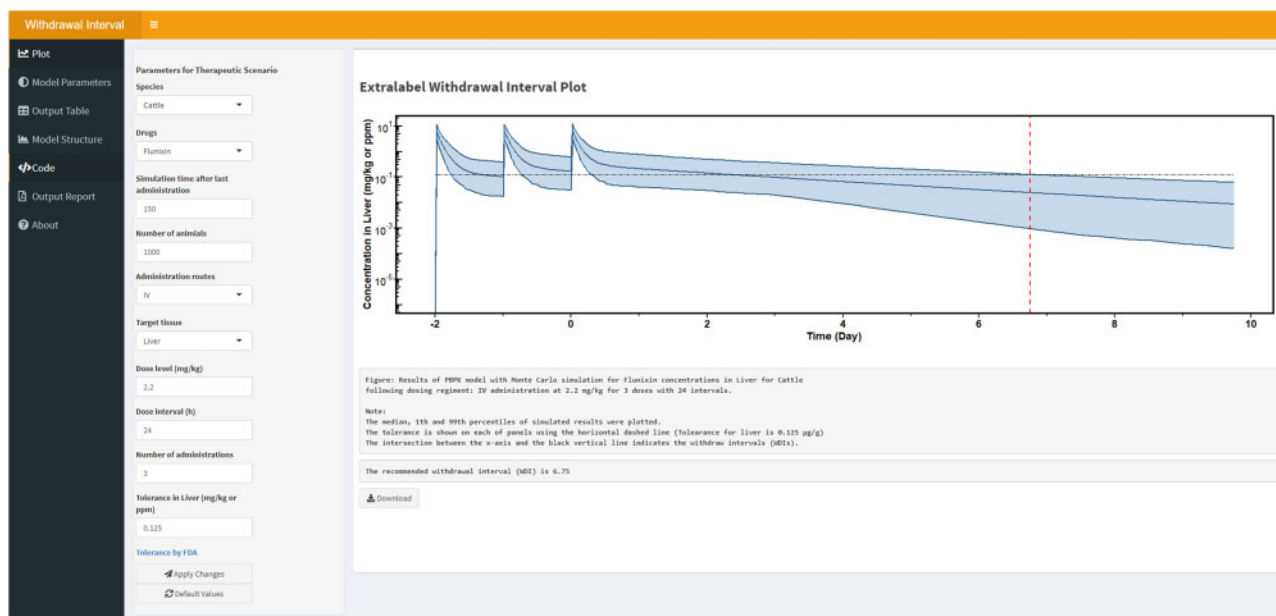


Figure 7. A screenshot of the developed web-based igPBPK interface for flunixin, florfenicol, and penicillin G in cattle and swine. This interface is available at: <http://pbpk.shinyapps.io/igPBPKApp>.

generic PBPK model in cattle (7 and 8 days for penicillin G and flunixin, respectively) and swine (11 and 14 days) were around 14%–45% different from the results in the previous models (ie, 5 and 6 days in cattle; 6 and 16 days in market-age swine). Based on the 5× label dose of penicillin G in swine, the current model-predicted WDI of 25 days was longer than ~9 days from the previous PBPK model for market-age swine (Halleran et al., 2022; Li et al., 2017) and shorter than 38 days from the previous PBPK model for heavy sows (Li et al., 2019b). The current population PBPK model was established based on not only the available datasets used in previous studies, but also new pharmacokinetic studies (Bates et al., 2020; Djebala et al., 2021; Kittrell et al., 2020; Li et al., 2019b) published after the development of the earlier PBPK models. Of note, the pharmacokinetic data for penicillin G from both market-age swine (Li et al., 2017) and heavy sows (Li et al., 2019b; Lupton et al., 2014) were incorporated into the present model to better capture the population variability. Consequently, the results from the current PBPK model for penicillin G in swine is somewhere between results from previous models for each of these production classes. Also, all physiological parameters in cattle and swine have been updated based on a recent comprehensive review article on physiological parameters for PBPK modeling in cattle and swine (Lin et al., 2020b), and variabilities of the fractional blood flows to liver and kidney in swine were larger than those in the earlier study (Li et al., 2017). Therefore, our model includes more variability and uncertainty from more comprehensive pharmacokinetic datasets and physiological parameters, resulting in a broad range of parameter values used in Monte Carlo simulations, which in turn contributes to more rigorous and conservative estimates of WDIs compared with the previous market-age swine model for penicillin G. It should be noted that these data represent penicillin G formulation complexed with procaine only, and not longer-acting formulations complexed with procaine and benzathine.

For florfenicol, commonly used extralabel administrations are 3 repeated IM injections at 20 mg/kg with 48-h intervals and 3 repeated SC injections at 40 mg/kg with 96-h intervals in cattle and 2 repeated SC injections at 40 mg/kg with a 96-h interval in

swine (Supplementary Table 9). The predicted extralabel WDIs were longer than FDA-approved label withdrawal times for SC administration in cattle (eg, predicted WDI was 48 days for 3 repeated SC doses at 40 mg/kg with 96-h intervals vs FDA-approved label withdrawal time of 38 days for a single SC dose) and in swine (eg, predicted WDI was 22 days for 2 repeated SC doses at 40 mg/kg with 96-h intervals vs FDA-approved label withdrawal time of 16 days for 5 daily dose via drinking water at 100 ppm), but it was close to FDA-approved label withdrawal times in the cattle model via IM injection (eg, predicted extralabel WDI 29 days vs label withdrawal time 28 days). These results indicate that violative residues might result following extralabel SC administrations in cattle and swine if the label withdrawal times are not extended substantially.

There are several limitations to this study. First, although the present PBPK model has successfully incorporated *in silico* mechanistic equations to predict partition coefficients of drugs based on physicochemical properties and tissue composition, the model does not include the prediction equations to estimate other critical model parameters such as the parameters related to protein binding, hepatic or renal clearance, and metabolism (Kamiya et al., 2019; Schneckener et al., 2019). Second, the development of the current PBPK model was mostly based on available pharmacokinetic data in market-age swine and adult cattle with only a few datasets in piglets, heavy sows, and calves (Li et al., 2019b; Lupton et al., 2014; Ranheim et al., 2002; Trolldenier et al., 1986). Although the simulation results adequately correspond to pharmacokinetics of all 3 selected drugs in different age groups of selected animal species, our model is not capable of considering the differences between ages, sexes, and production classes. Additional data, especially the physiological and anatomical data in different ages and sexes, can be incorporated into the model to enhance the predictability and ensure the model is as close to reality as possible. Recently, our group has published a series of studies to establish a database of physiological parameters for developing PBPK models for drugs and environmental chemicals in different food-producing animals, including cattle and swine (Lin et al., 2020b), chickens and

turkeys (Wang et al., 2021), and sheep and goats (Li et al., 2021). Based on this physiological parameter database, the present igPBPK modeling platform can be extended to other food animal species in the future. Third, while the CV values of chemical-specific values were based on default assumptions that are generally acceptable to be conservative in the field of PBPK modeling (Henri et al., 2017; Li et al., 2017; Riad et al., 2021; Yang et al., 2015), there are inevitably some uncertainty associated with these parameters. Additional experimental studies that directly measure the CV values of these parameters will help improve the present model. Fourth, the present study only did a local sensitivity analysis, which does not consider interactions between parameters. Global sensitivity analysis (Hsieh et al., 2018; McNally et al., 2011; Tardiveau et al., 2022) should be performed in order to assess the relative sensitivities of model parameters and their interactions in the future. Finally, the current model was developed so that it could predict WDIs for 3 different drugs when given individually, but it does not specifically predict WDIs when these 3 drugs are given concurrently because the model does not account for potential drug-drug interactions.

## CONCLUSIONS

This study reports a new interactive generic PBPK modeling platform for multiple drugs in cattle and swine that can be used in real-time field exposure scenarios. This modeling platform has been implemented to build PBPK models for 3 representative drugs (flunixin, florfenicol, and penicillin G) in both species. Model simulations, in general, are in good agreement with the observed concentrations of flunixin, 5-hydroxy flunixin, florfenicol, florfenicol amine, and penicillin G residues in edible tissues of cattle and swine after different exposure regimens. Predictions of WDIs for FDA-approved label use and common extralabel uses of the 3 selected drugs using the population PBPK model with Monte Carlo simulations demonstrate the ability of the model to provide more protective WDI recommendations to help ensure safety of food products derived from animals treated with these drugs under field dosing conditions. The final generic PBPK model has been converted to a web-based igPBPK interface to provide a user-friendly platform to facilitate the application of this PBPK modeling platform for users with or without computer programming experiences. Although this model still has some limitations, the igPBPK framework represents a proof-of-concept toward the next-generation PBPK model and provides a robust foundational tool to extrapolate to other drugs and other food animal species.

## SUPPLEMENTARY DATA

Supplementary data are available at *Toxicological Sciences* online.

## DECLARATION OF CONFLICTING INTERESTS

The authors declare no conflict of interest.

## FUNDING INFORMATION

This work was supported by the U.S. Department of Agriculture (USDA) National Institute of Food and Agriculture (NIFA) for the FARAD Program (Award Nos. 2019-41480-30296, 2020-41480-32497, and 2021-41480-35271).

## ACKNOWLEDGMENTS

The authors would like to acknowledge Dr. Long Yuan, Dr. Md Mahbubul Huq Riad, and Dr. Qiran Chen from the Center for Environmental and Human Toxicology, Department of Environmental and Global Health, College of Public Health and Health Professions, University of Florida for helpful discussions.

## REFERENCES

- Adams, P. E., Varma, K. J., Powers, T. E., and Lamendola, J. F. (1987). Tissue concentrations and pharmacokinetics of florfenicol in male veal calves given repeated doses. *Am. J. Vet. Res.* **48**, 1725–1732.
- Aksu, M. I., Dogan, M., and Sirkecioglu, A. N. (2017). Changes in the total lipid, neutral lipid, phospholipid and fatty acid composition of phospholipid fractions during pastirma processing, a dry-cured meat product. *Korean J. Food Sci. Anim. Resour.* **37**, 18–28.
- Baron, K. T., and Gastonguay, M. R. (2015). Simulation from ODE-based population PK/PD and systems pharmacology models in R with mrgsolve. *J. Pharmacokinet. Phar.* **42**, S84–S85.
- Bates, J. L., Karriker, L. A., Rajewski, S. M., Lin, Z., Gehring, R., Li, M., Riviere, J. E., and Coetzee, J. F. (2020). A study to assess the correlation between plasma, oral fluid and urine concentrations of flunixin meglumine with the tissue residue depletion profile in finishing-age swine. *BMC Vet. Res.* **16**, 211.
- Baynes, R. E., Dedonder, K., Kissell, L., Mzyk, D., Marmulak, T., Smith, G., Tell, L., Gehring, R., Davis, J., and Riviere, J. E. (2016). Health concerns and management of select veterinary drug residues. *Food Chem. Toxicol.* **88**, 112–122.
- Berezhkovskiy, L. M. (2004). Volume of distribution at steady state for a linear pharmacokinetic system with peripheral elimination. *J. Pharm. Sci.* **93**, 1628–1640.
- Bretzlaff, K. N., Neff-Davis, C. A., Ott, R. S., Koritz, G. D., Gustafsson, B. K., and Davis, L. E. (1987). Florfenicol in non-lactating dairy cows: Pharmacokinetics, binding to plasma proteins, and effects on phagocytosis by blood neutrophils. *J. Vet. Pharmacol. Ther.* **10**, 233–240.
- Buur, J. L., Baynes, R. E., Smith, G., and Riviere, J. E. (2006). Pharmacokinetics of flunixin meglumine in swine after intravenous dosing. *J. Vet. Pharmacol. Ther.* **29**, 437–440.
- Canton, L., Lanusse, C., and Moreno, L. (2021). Rational pharmacotherapy in infectious diseases: Issues related to drug residues in edible animal tissues. *Animals (Basel)* **11**, 2878.
- Chiesa, O. A., Von Bredow, J., Smith, M., Heller, D., Condon, R., and Thomas, M. H. (2006). Bovine kidney tissue/biological fluid correlation for penicillin. *J. Vet. Pharmacol. Ther.* **29**, 299–306.
- Chou, W. C., and Lin, Z. (2019). Bayesian evaluation of a physiologically based pharmacokinetic (PBPK) model for perfluorooctane sulfonate (PFOS) to characterize the interspecies uncertainty between mice, rats, monkeys, and humans: Development and performance verification. *Environ. Int.* **129**, 408–422.
- Chou, W. C., and Lin, Z. (2020). Probabilistic human health risk assessment of perfluorooctane sulfonate (PFOS) by integrating in vitro, in vivo toxicity, and human epidemiological studies using a Bayesian-based dose-response assessment coupled with physiologically based pharmacokinetic (PBPK) modeling approach. *Environ. Int.* **137**, 105581.
- Chou, W. C., and Lin, Z. (2021). Development of a gestational and lactational physiologically based pharmacokinetic (PBPK)

- model for perfluorooctane sulfonate (PFOS) in rats and humans and its implications in the derivation of health-based toxicity values. *Environ. Health Persp.* **129**, 37004.
- Croubels, S., Baert, K., Verheyen, T., Boone, G., and De Backer, P. (2006). Pharmacokinetics and oral bioavailability of florfenicol in veal calves. *J. Vet. Pharmacol. Ther.* **29**, 104–105.
- Cully, M. (2014). Public health the politics of antibiotics. *Nature* **509**, S16–S17.
- de Craene, B. A., Deprez, P., D'Haese, E., Nelis, H. J., Van den Bossche, W., and De Leenheer, P. (1997). Pharmacokinetics of florfenicol in cerebrospinal fluid and plasma of calves. *Antimicrob. Agents Chemother.* **41**, 1991–1995.
- Djebala, S., Croubels, S., Cherlet, M., Martinelle, L., Thiry, D., Moula, N., Sartelet, A., and Bossaert, P. (2021). Description of plasma penicillin G concentrations after intramuscular injection in double-musled cows to optimize the timing of antibiotherapy for caesarean section. *Vet. Sci.* **8**, 67.
- Durso, L. M., and Cook, K. L. (2014). Impacts of antibiotic use in agriculture: What are the benefits and risks? *Curr. Opin. Microbiol.* **19**, 37–44.
- EMA. (1999). Committee for veterinary medicinal products flunixin summary reports (1). The European Medicines Agency (EMA). Available at: [http://www.ema.europa.eu/docs/en\\_gb/document\\_library/maximum\\_residue\\_limits\\_-\\_report/2009/11/wc500014324.pdf](http://www.ema.europa.eu/docs/en_gb/document_library/maximum_residue_limits_-_report/2009/11/wc500014324.pdf). Accessed November 14, 2021.
- Embrechts, J., Sedlák, L., Hlavizna, I., Heřmanský, P., Čechová, I., Brožková, M., Beránková, A., and De Busser, J. (2013). The influence of the galenic form on pharmacokinetics of florfenicol after intramuscular administration in pigs. *J. Vet. Pharmacol. Ther.* **36**, 92–94.
- FDA. (1998). Freedom of information. NADA 101-479. Banamine (flunixin meglumine) injectable solution. US Food and Drug Administration, Silver Spring, MD. Available at: <https://wayback.archive-it.org/7993/20170406083138/https://www.fda.gov/downloads/animalveterinary/products/approvedanimaldrugproducts/foiadrugsummaries/ucm064905.pdf>. Accessed November 14, 2021.
- FDA. (2005). BANAMINE-S (flunixin meglumine) injectable solution. U.S. Food and Drug Administration, Silver Spring, MD. Freedom of Information. NADA 101. Available at: <https://animaldrugsatfda.fda.gov/adafda/app/search/public/document/downloadFoi/356>. Accessed November 14, 2021.
- FDA. (2018). General principles for evaluating the human food safety of new animal drugs used in food-producing animals—guidance for industry. U.S. Food and Drug Administration, Rockville, MD. Available at: <https://www.fda.gov/media/70028/download>. Accessed December 2, 2021.
- FDA. (2020). Title 21—food and drugs chapter I. Food and Drug Administration sec. 556.283 Florfenicol, Silver Spring, MD. Available at: <https://www.accessdata.fda.gov/scripts/cdrh/cfdocs/cfcfr/cfrsearch.cfm?Fr=556.283>. Accessed November 14, 2021.
- Galbraith, E. A., and McKellar, Q. A. (1996). Protein binding and in vitro serum thromboxane B2 inhibition by flunixin meglumine and meclofenamic acid in dog, goat and horse blood. *Res. Vet. Sci.* **61**, 78–81.
- Gilliam, J. N., Streeter, R. N., Papich, M. G., Washburn, K. E., and Payton, M. E. (2008). Pharmacokinetics of florfenicol in serum and synovial fluid after regional intravenous perfusion in the distal portion of the hind limb of adult cows. *Am. J. Vet. Res.* **69**, 997–1004.
- Halleran, J. L., Papich, M. G., Li, M., Lin, Z., Davis, J. L., Maunsell, F. P., Riviere, J. E., Baynes, R. E., and Foster, D. M. (2022). Update on withdrawal intervals following extralabel use of procaine penicillin G in cattle and swine. *J. Am. Vet. Med. Assoc.* **260**, 50–56.
- Haritova, A. M., and Fink-Gremmels, J. (2010). A simulation model for the prediction of tissue: Plasma partition coefficients for drug residues in natural casings. *Vet. J.* **185**, 278–284.
- Henri, J., Carrez, R., Meda, B., Laurentie, M., and Sanders, P. (2017). A physiologically based pharmacokinetic model for chickens exposed to feed supplemented with monensin during their lifetime. *J. Vet. Pharmacol. Ther.* **40**, 370–382.
- Howard, J. T., Baynes, R. E., Brooks, J. D., Yeatts, J. L., Bellis, B., Ashwell, M. S., Routh, P., O'Nan, A. T., and Maltecca, C. (2014). The effect of breed and sex on sulfamethazine, enrofloxacin, fenbendazole and flunixin meglumine pharmacokinetic parameters in swine. *J. Vet. Pharmacol. Ther.* **37**, 531–541.
- Hsieh, N. H., Reifeld, B., Bois, F. Y., and Chiu, W. A. (2018). Applying a global sensitivity analysis workflow to improve the computational efficiencies in physiologically-based pharmacokinetic modeling. *Front. Pharmacol.* **9**, 588.
- Intervet Inc. (2009). Freedom of information summary: Original new animal drug application. NADA 141-299, resflor gold: Florfenicol and flunixin meglumine (in 2-pyrrolidone and triacetin) injectable solution beef and non-lactating dairy cattle. Available at: <http://cafarad.ucdavis.edu/citationsearch/searchcitations/9014087.pdf>. Accessed October 30, 2021.
- Jaroszewski, J., Jedziniak, P., Markiewicz, W., Grabowski, T., Chrostowska, M., and Szprengier-Juszkiewicz, T. (2008). Pharmacokinetics of flunixin in mature heifers following multiple intravenous administration. *Pol. J. Vet. Sci.* **11**, 199–203.
- Jiang, H. X., Zeng, Z. L., Chen, Z. L., Liu, J. J., and Fung, K. F. (2006). Pharmacokinetics of florfenicol in pigs following intravenous, intramuscular or oral administration and the effects of feed intake on oral dosing. *J. Vet. Pharmacol. Ther.* **29**, 153–156.
- Kamiya, Y., Otsuka, S., Miura, T., Takaku, H., Yamada, R., Nakazato, M., Nakamura, H., Mizuno, S., Shono, F., Funatsu, K., et al. (2019). Plasma and hepatic concentrations of chemicals after virtual oral administrations extrapolated using rat plasma data and simple physiologically based pharmacokinetic models. *Chem. Res. Toxicol.* **32**, 792–792.
- Kim, M. H., Gebru, E., Chang, Z. Q., Choi, J. Y., Hwang, M. H., Kang, E. H., Lim, J. H., Yun, H. I., and Park, S. C. (2008). Comparative pharmacokinetics of tylosin or florfenicol after a single intramuscular administration at two different doses of tylosin-florfenicol combination in pigs. *J. Vet. Med. Sci.* **70**, 99–102.
- Kissell, L. W., Brinson, P. D., Gehring, R., Tell, L. A., Wetzlich, S. E., Baynes, R. E., Riviere, J. E., and Smith, G. W. (2016). Pharmacokinetics and tissue elimination of flunixin in veal calves. *Am. J. Vet. Res.* **77**, 634–640.
- Kittrell, H. C., Mochel, J. P., Brown, J. T., Forseth, A. M. K., Hayman, K. P., Rajewski, S. M., Coetzee, J. F., Schneider, B. K., Ratliffe, B., Skoland, K. J., et al. (2020). Pharmacokinetics of intravenous, intramuscular, oral, and transdermal administration of flunixin meglumine in pre-wean piglets. *Front. Vet. Sci.* **7**, 586.
- Kleinhenz, M. D., Van Engen, N. K., Gorden, P. J., Kukanich, B., Rajewski, S. M., Walsh, P., and Coetzee, J. F. (2016). The pharmacokinetics of transdermal flunixin meglumine in holstein calves. *J. Vet. Pharmacol. Ther.* **39**, 612–615.
- Korsrud, G. O., Boison, J. O., Papich, M. G., Yates, W. D., MacNeil, J. D., Janzen, E. D., Cohen, R. D., Landry, D. A., Lambert, G., and Yong, M. S. (1993). Depletion of intramuscularly and subcutaneously injected procaine penicillin G from tissues and plasma of yearling beef steers. *Can. J. Vet. Res.* **57**, 223–230.

- Korsrud, G. O., Salisbury, C. D. C., Rhodes, C. S., Papich, M. G., Yates, W. D. G., Bulmer, W. S., MacNeil, J. D., Landry, D. A., Lambert, G., Yong, M. S., et al. (1998). Depletion of penicillin G residues in tissues, plasma and injection sites of market pigs injected intramuscularly with procaine penicillin G. *Food Addit. Contam.* **15**, 421–426.
- KuKanich, B., Gehring, R., Webb, A. I., Craigmill, A. L., and Riviere, J. E. (2005). Effect of formulation and route of administration on tissue residues and withdrawal times. *J. Am. Vet. Med. Assoc.* **227**, 1574–1577.
- Lacroix, M. Z., Gayrard, V., Picard-Hagen, N., and Toutain, P. L. (2011). Comparative bioavailability between two routes of administration of florfenicol and flunixin in cattle. *Rev. Med. Vet.* **162**, 321–324.
- Lautz, L. S., Nebbia, C., Hoeks, S., Oldenkamp, R., Hendriks, A. J., Ragas, A. M. J., and Dorne, J. L. C. M. (2020). An open source physiologically based kinetic model for the chicken (*Gallus gallus domesticus*): Calibration and validation for the prediction residues in tissues and eggs. *Environ. Int.* **136**, 105488.
- Law, F. C. P. (1999). A physiologically based pharmacokinetic model for predicting the withdrawal period of oxytetracycline in cultured chinook salmon (*Oncorhynchus tshawytscha*). In *Xenobiotics in Fish* (D. Smith, W. H. Gingerich, and M. G. Beconi-Barker, Eds.), pp. 105–121. Kluwer Academic/Plenum Publishers, New York.
- Lei, Z. X., Liu, Q. Y., Yang, S. K., Yang, B., Khaliq, H., Li, K., Ahmed, S., Sajid, A., Zhang, B. Z., Chen, P., et al. (2018). PK–PD integration modeling and cutoff value of florfenicol against *Streptococcus suis* in pigs. *Front. Pharmacol.* **9**, 2.
- Li, J. Z., Fung, K. F., Chen, Z. L., Zeng, Z. L., and Zhang, J. (2002). Tissue pharmacokinetics of florfenicol in pigs experimentally infected with *Actinobacillus pleuropneumoniae*. *Eur. J. Drug Metab. Pharmacokin.* **27**, 265–271.
- Li, M., Cheng, Y. H., Chittenden, J. T., Baynes, R. E., Tell, L. A., Davis, J. L., Vickroy, T. W., Riviere, J. E., and Lin, Z. (2019a). Integration of Food Animal Residue Avoidance Databank (FARAD) empirical methods for drug withdrawal interval determination with a mechanistic population-based interactive physiologically based pharmacokinetic (ipbpk) modeling platform: Example for flunixin meglumine administration. *Arch. Toxicol.* **93**, 1865–1880.
- Li, M., Gehring, R., Riviere, J. E., and Lin, Z. (2017). Development and application of a population physiologically based pharmacokinetic model for penicillin G in swine and cattle for food safety assessment. *Food Chem. Toxicol.* **107**, 74–87.
- Li, M., Gehring, R., Riviere, J. E., and Lin, Z. (2018). Probabilistic physiologically based pharmacokinetic model for penicillin G in milk from dairy cows following intramammary or intramuscular administrations. *Toxicol. Sci.* **164**, 85–100.
- Li, M., Mainquist-Whigham, C., Karriker, L. A., Wulf, L. W., Zeng, D. P., Gehring, R., Riviere, J. E., Coetzee, J. F., and Lin, Z. (2019b). An integrated experimental and physiologically based pharmacokinetic modeling study of penicillin G in heavy sows. *J. Vet. Pharmacol. Ther.* **42**, 461–475.
- Li, M., Wang, Y. S., Elwell-Cuddy, T., Baynes, R. E., Tell, L. A., Davis, J. L., Maunsell, F. P., Riviere, J. E., and Lin, Z. (2021). Physiological parameter values for physiologically based pharmacokinetic models in food-producing animals. Part III: Sheep and goat. *J. Vet. Pharmacol. Ther.* **44**, 456–477.
- Lin, Z., Fisher, J. W., Wang, R., Ross, M. K., and Filipov, N. M. (2013). Estimation of placental and lactational transfer and tissue distribution of atrazine and its main metabolites in rodent dams, fetuses, and neonates with physiologically based pharmacokinetic modeling. *Toxicol. Appl. Pharm.* **273**, 140–158.
- Lin, Z., Gehring, R., Mochel, J. P., Lave, T., and Riviere, J. E. (2016a). Mathematical modeling and simulation in animal health—Part II: Principles, methods, applications, and value of physiologically based pharmacokinetic modeling in veterinary medicine and food safety assessment. *J. Vet. Pharmacol. Ther.* **39**, 421–438.
- Lin, Z., Jaber-Douraki, M., He, C., Jin, S., Yang, R. S. H., Fisher, J. W., and Riviere, J. E. (2017). Performance assessment and translation of physiologically based pharmacokinetic models from acsLX to Berkeley Madonna, MATLAB, and R language: Oxytetracycline and gold nanoparticles as case examples. *Toxicol. Sci.* **158**, 23–35.
- Lin, Z., Li, M., Baynes, R. E., Tell, L. A., Davis, J. L., Vickroy, T. W., and Riviere, J. E. (2020a). Development and application of an interactive physiologically based pharmacokinetic (iPBPK) model interface to estimate withdrawal intervals for penicillin G in cattle and swine. The 59th Annual Meeting of Society of Toxicology, Anaheim, California. The toxicologist, Supplement to Toxicological Sciences, Vol. 174, p. 458 (Abstract #2932).
- Lin, Z., Li, M., Wang, Y. S., Tell, L. A., Baynes, R. E., Davis, J. L., Vickroy, T. W., and Riviere, J. E. (2020b). Physiological parameter values for physiologically based pharmacokinetic models in food-producing animals. Part I: Cattle and swine. *J. Vet. Pharmacol. Ther.* **43**, 385–420.
- Lin, Z., Li, M. J., Gehring, R., and Riviere, J. E. (2015). Development and application of a multiroute physiologically based pharmacokinetic model for oxytetracycline in dogs and humans. *J. Pharm. Sci.* **104**, 233–243.
- Lin, Z., Monteiro-Riviere, N. A., and Riviere, J. E. (2016b). A physiologically based pharmacokinetic model for polyethylene glycol-coated gold nanoparticles of different sizes in adult mice. *Nanotoxicology* **10**, 162–172.
- Liu, J., Fung, K. F., Chen, Z., Zeng, Z., and Zhang, J. (2003). Pharmacokinetics of florfenicol in healthy pigs and in pigs experimentally infected with *Actinobacillus pleuropneumoniae*. *Antimicrob. Agents Chemother.* **47**, 820–823.
- Lobell, R. D., Varma, K. J., Johnson, J. C., Sams, R. A., Gerken, D. F., and Ashcraft, S. M. (1994). Pharmacokinetics of florfenicol following intravenous and intramuscular doses to cattle. *J. Vet. Pharmacol. Ther.* **17**, 253–258.
- Lupton, S. J., Shelver, W. L., Newman, D. J., Larsen, S., and Smith, D. J. (2014). Depletion of penicillin G residues in heavy sows after intramuscular injection. Part I: Tissue residue depletion. *J. Agric. Food Chem.* **62**, 7577–7585.
- McNally, K., Cotton, R., and Loizou, G. D. (2011). A workflow for global sensitivity analysis of PBPK models. *Front. Pharmacol.* **2**, 31.
- Mirfazaelian, A., Kim, K. B., Anand, S. S., Kim, H. J., Tornero-Velez, R., Bruckner, J. V., and Fisher, J. W. (2006). Development of a physiologically based pharmacokinetic model for deltamethrin in the adult male Sprague-Dawley rat. *Toxicol. Sci.* **93**, 432–442.
- Norbrook Laboratories, L. (2015). Freedom of information summary: Original abbreviated new animal drug application NADA 200-591. Norfenicol florfenicol injectable solution beef and non-lactating dairy cattle. FARAD Reference Number: 9016669.
- NRC. (1999). The use of drugs in food animals. In *The Use of Drugs in Food Animals: Benefits and Risks* (Council NR, Ed.), pp 110–141. National Academy Press, Washington, DC.
- Odensvik, K. (1995). Pharmacokinetics of flunixin and its effect on prostaglandin-F<sub>2</sub>-alpha metabolite concentrations after



- oral and intravenous administration in heifers. *J. Vet. Pharmacol. Ther.* **18**, 254–259.
- Odensvik, K., and Johansson, I. M. (1995). High-performance liquid-chromatography method for determination of flunixin in bovine plasma and pharmacokinetics after single and repeated doses of the drug. *Am. J. Vet. Res.* **56**, 489–495.
- OECD. (2021). Guidance document on the characterisation, validation and reporting of physiologically based kinetic (PBK) models for regulatory purposes, OECD Series on Testing and Assessment, No. 331, Environment, Health and Safety, Environment Directorate, Organisation for Economic Co-operation and Development (OECD). Available at: <https://www.oecd.org/chemicalsafety/risk-assessment/guidance-document-on-the-characterisation-validation-and-reporting-of-physiologically-based-kinetic-models-for-regulatory-purposes.pdf>. Accessed May 30, 2022.
- Pairis-Garcia, M. D., Karriker, L. A., Johnson, A. K., Kukanich, B., Wulf, L., Sander, S., Millman, S. T., Stalder, K. J., and Coetzee, J. F. (2013). Pharmacokinetics of flunixin meglumine in mature swine after intravenous, intramuscular and oral administration. *BMC Vet. Res.* **9**, 165.
- Papich, M. G., Korsrud, G. O., Boison, J. O., Yates, W. D., MacNeil, J. D., Janzen, E. D., Cohen, R. D., and Landry, D. A. (1993). A study of the disposition of procaine penicillin G in feedlot steers following intramuscular and subcutaneous injection. *J. Vet. Pharmacol. Ther.* **16**, 317–327.
- Peterson, L. R. (1978). Quantitative binding of penicillin-G to tissue-homogenates as determined with preparative ultracentrifuge. *J. Lab. Clin. Med.* **91**, 463–466.
- Poulin, P., Collet, S. H., Atrux-Tallau, N., Linget, J. M., Hennequin, L., and Wilson, C. E. (2019). Application of the tissue composition-based model to minipig for predicting the volume of distribution at steady state and dermis-to-plasma partition coefficients of drugs used in the physiologically based pharmacokinetics model in dermatology. *J. Pharm. Sci.* **108**, 603–619.
- Poulin, P., and Theil, F. P. (2002). Prediction of pharmacokinetics prior to in vivo studies. 1. Mechanism-based prediction of volume of distribution. *J. Pharm. Sci.* **91**, 129–156.
- Ranheim, B., Ween, H., Egeli, A. K., Hormazabal, V., Yndestad, M., and Soli, N. E. (2002). Benzathine penicillin G and procaine penicillin G in piglets: Comparison of intramuscular and subcutaneous injection. *Vet. Res. Commun.* **26**, 459–465.
- Riad, M. H., Baynes, R. E., Tell, L. A., Davis, J. L., Maunsell, F. P., Riviere, J. E., and Lin, Z. (2021). Development and application of an interactive physiologically based pharmacokinetic (iPBPK) model to predict oxytetracycline tissue distribution and withdrawal intervals in market-age sheep and goats. *Toxicol. Sci.* **183**, 253–268.
- Riviere, J. E., Tell, L. A., Baynes, R. E., Vickroy, T. W., and Gehring, R. (2017). Guide to farad resources: Historical and future perspectives. *J. Am. Vet. Med. Assoc.* **250**, 1131–1139.
- Rodgers, T., Leahy, D., and Rowland, M. (2005). Physiologically based pharmacokinetic modeling 1: Predicting the tissue distribution of moderate-to-strong bases. *J. Pharm. Sci.* **94**, 1259–1276.
- Rodgers, T., and Rowland, M. (2006). Physiologically based pharmacokinetic modelling 2: Predicting the tissue distribution of acids, very weak bases, neutrals and zwitterions. *J. Pharm. Sci.* **95**, 1238–1257.
- Schmitt, W. (2008). General approach for the calculation of tissue to plasma partition coefficients. *Toxicol. In Vitro* **22**, 457–467.
- Schneckener, S., Grimbs, S., Hey, J., Menz, S., Osmers, M., Schaper, S., Hillisch, A., and Goller, A. H. (2019). Prediction of oral bioavailability in rats: Transferring insights from in vitro correlations to (deep) machine learning models using in silico model outputs and chemical structure parameters. *J. Chem. Inf. Model.* **59**, 4893–4905.
- Shelver, W. L., Tell, L. A., Wagner, S., Wetzlich, S. E., Baynes, R. E., Riviere, J. E., and Smith, D. J. (2013). Comparison of ELISA and LC-MS/MS for the measurement of flunixin plasma concentrations in beef cattle after intravenous and subcutaneous administration. *J. Agr. Food Chem.* **61**, 2679–2686.
- Sidhu, P., Rassouli, A., Illambas, J., Potter, T., Pelligand, L., Rycroft, A., and Lees, P. (2014). Pharmacokinetic-pharmacodynamic integration and modelling of florfenicol in calves. *J. Vet. Pharmacol. Ther.* **37**, 231–242.
- Singh, A. V., Ansari, M. H. D., Rosenkranz, D., Maharjan, R. S., Kriegel, F. L., Gandhi, K., Kanase, A., Singh, R., Laux, P., and Luch, A. (2020). Artificial intelligence and machine learning in computational nanotoxicology: Unlocking and empowering nanomedicine. *Adv. Healthc. Mater.* **9**, 1901862.
- SPAHC. (2002). Freedom of information summary: Original abbreviated new animal drug application. NADA 141–206. Nuflor 2.3% Concentrate Solution. Schering-Plough Animal Health Corporation (SPAHC). Available at: <https://animal-drugsatfda.fda.gov/adafda/app/search/public/document/downloadFoi/724>. Accessed May 30, 2022.
- SPAHC. (2006). Freedom of information summary, supplemental new animal drug application. NADA 141-063, Nuflor injectable solution, forfenicol injectable solution, cattle. Schering-Plough Animal Health Corporation (SPAHC). Available at: <http://cafarad.Ucdavis.Edu/citationsearch/searchcitations/9014514.Pdf>. Accessed November 14, 2021.
- SPAHC. (2008). Freedom of information summary: Original new animal drug application. NADA 141-265. Nuflor gold injectable solution. Florfenicol (with 2-pyrrolidone and triacetin) for beef and non-lactating dairy cattle. Schering-Plough Animal Health Corporation (SPAHC). FARAD Reference Number: 914686.
- Tan, Y. M., Worley, R. R., Leonard, J. A., and Fisher, J. W. (2018). Challenges associated with applying physiologically based pharmacokinetic modeling for public health decision-making. *Toxicol. Sci.* **162**, 341–348.
- Tardiveau, J., LeRoux-Pullen, L., Gehring, R., Touchais, G., Chotard-Soutif, M. P., Mirfendereski, H., Paraud, C., Jacobs, M., Magnier, R., Laurentie, M., et al. (2022). A physiologically based pharmacokinetic (PBPK) model exploring the blood-milk barrier in lactating species - a case study with oxytetracycline administered to dairy cows and goats. *Food Chem. Toxicol.* **161**, 112848.
- Trolldenier, H., Ratzinger, S., Bache, K., Amm, H., and Dubrow, R. (1986). Blood-levels, pharmacokinetics, and residualization of benzylpenicillins (Ursopen 100000) in calves, following subcutaneous injection. *Monatsh. Veterinarmed.* **41**, 435–441.
- USDA. (2013). Screening and confirmation of animal drug residues by UHPLC-MS-MS. Available at: [https://www.Fsis.USda.Gov/sites/default/files/media\\_file/2020-09/clg-mrm1.Pdf](https://www.Fsis.USda.Gov/sites/default/files/media_file/2020-09/clg-mrm1.Pdf). Accessed November 14, 2021.
- Utsey, K., Gastonguay, M. S., Russell, S., Freling, R., Riggs, M. M., and Elmokadem, A. (2020). Quantification of the impact of partition coefficient prediction methods on physiologically based pharmacokinetic model output using a standardized tissue composition. *Drug Metab. Dispos.* **48**, 903–916.
- Vanselow, B., and Griffith, G. (2001). The use of drugs in food animals: Benefits and risks. *Aust. J. Agr. Resour. Econ.* **45**, 641–643.

- Varma, K. J., Adams, P. E., Powers, T. E., Powers, J. D., and Lamendola, J. F. (1986). Pharmacokinetics of florfenicol in veal calves. *J. Vet. Pharmacol. Ther.* **9**, 412–425.
- Voorspoels, J., D'Haese, E., de Craene, B. A., Vervaeke, C., de Riemaecker, D., Deprez, P., Nelis, H., and Remon, J. P. (1999). Pharmacokinetics of florfenicol after treatment of pigs with single oral or intramuscular doses or with medicated feed for three days. *Vet. Rec.* **145**, 397–399.
- Wang, Y. S., Li, M., Tell, L. A., Baynes, R. E., Davis, J. L., Vickroy, T. W., Riviere, J. E., and Lin, Z. (2021). Physiological parameter values for physiologically based pharmacokinetic models in food-producing animals. Part II: Chicken and turkey. *J. Vet. Pharmacol. Ther.* **44**, 423–455.
- WHO. (2010). Characterization and application of physiologically based pharmacokinetic models in risk assessment, pp. 1–91. World Health Organization (WHO), International Programme on Chemical Safety, Geneva, Switzerland. Available at: <https://apps.who.int/iris/handle/10665/44495>. Accessed November 14, 2021.
- Yang, F., Lin, Z., Riviere, J. E., and Baynes, R. E. (2019). Development and application of a population physiologically based pharmacokinetic model for florfenicol and its metabolite florfenicol amine in cattle. *Food Chem. Toxicol.* **126**, 285–294.
- Yang, X. X., Doerge, D. R., Teeguarden, J. G., and Fisher, J. W. (2015). Development of a physiologically based pharmacokinetic model for assessment of human exposure to bisphenol A. *Toxicol. Appl. Pharm.* **289**, 442–456.
- Zeng, D., Lin, Z., Zeng, Z., Fang, B., Li, M., Cheng, Y. H., and Sun, Y. (2019). Assessing global human exposure to T-2 toxin via poultry meat consumption using a lifetime physiologically based pharmacokinetic model. *J. Agric. Food Chem.* **67**, 1563–1571.
- Zhang, Q., Tang, S. S., Qian, M. Y., Wei, L., Zhou, D., Zhang, Z. J., He, J. K., Zhang, Q. J., Zhu, P., and Xiao, X. L. (2016). Nanoemulsion formulation of florfenicol improves bioavailability in pigs. *J. Vet. Pharmacol. Ther.* **39**, 84–89.
- Zhou, K., Liu, A., Ma, W., Sun, L., Mi, K., Xu, X., Algharib, S. A., Xie, S., and Huang, L. (2021). Apply a physiologically based pharmacokinetic model to promote the development of enrofloxacin granules: Predict withdrawal interval and toxicity dose. *Antibiotics (Basel)* **10**, 955.